

FEDERAL RESERVE BANK OF SAN FRANCISCO

WORKING PAPER SERIES

## **Replicating Business Cycles and Asset Returns with Sentiment and Low Risk Aversion**

Kevin Lansing  
Federal Reserve Bank of San Francisco

July 2024

Working Paper 2021-02

<https://doi.org/10.24148/wp2021-02>

**Suggested citation:**

Lansing, Kevin. 2024. “Replicating Business Cycles and Asset Returns with Sentiment and Low Risk Aversion.” Federal Reserve Bank of San Francisco Working Paper 2021-02. <https://doi.org/10.24148/wp2021-02>

The views in this paper are solely the responsibility of the authors and should not be interpreted as reflecting the views of the Federal Reserve Bank of San Francisco or the Board of Governors of the Federal Reserve System.

# Replicating Business Cycles and Asset Returns with Sentiment and Low Risk Aversion\*

Kevin J. Lansing<sup>†</sup>  
Federal Reserve Bank of San Francisco

July 25, 2024

## Abstract

I solve for the sequences of shocks (or wedges) that allow a standard real business cycle model to exactly replicate the quarterly time paths of U.S. macroeconomic variables and asset returns since 1960. The resulting shock sequences can be grouped into three main categories: (1) shocks that affect household sentiment and preferences, (2) shocks that appear in the law of motion for capital, and (3) shocks that appear in the production function for output. For most variables including output, no single shock category is clearly dominant in explaining the observed movements in U.S. data. While some variables are driven by a single dominant shock category, the dominant category is different for each of those variables. The results imply that there is no “most important shock.” Rather, U.S. economic outcomes have been shaped by a complex and time-varying mixture of fundamental and non-fundamental disturbances.

Keywords: *Business cycle accounting, Sentiment, Animal spirits, Risk aversion, Equity risk premium, Bond term premium.*

JEL Classification: E32, E44, O41.

---

\*Forthcoming in *Journal of Economic Dynamics and Control*. I thank Michal Andrle, Steve LeRoy, Jun Ma, numerous conference participants, and two anonymous referees whose comments and suggestions significantly improved this article. Any views expressed here do not necessarily reflect the views of the Federal Reserve of Bank of San Francisco or the Board of Governors of the Federal Reserve System.

<sup>†</sup>Research Department, Federal Reserve Bank of San Francisco, P.O. Box 7702, San Francisco, CA 94120-7702, kevin.j.lansing@sf.frb.org

# 1 Introduction

The macroeconomics literature has not reached a consensus in identifying the most important forces driving U.S. business cycles. Chari, Kehoe, and McGrattan (2007) conclude that “efficiency wedges” (e.g., labor productivity shocks) and “labor supply wedges” (e.g., labor disutility shocks) are the main drivers of business cycles. Smets and Wouters (2007) find that shocks to labor productivity and wage mark-ups account for most of the fluctuations in output over the medium- to long-run. Justiniano, Primiceri, and Tambalotti (2010) conclude that an “investment shock” which appears in the law of motion for capital is the main driver of business cycle fluctuations in output, hours, and investment. Christiano, Motto, and Rostagno (2014) conclude that “risk shocks” (defined as the time-varying volatility of firms’ idiosyncratic productivity realizations) are the most important business cycle shocks. Miao, Wang, and Xu (2015) find that a “sentiment shock” (which influences the size of a rational stock price bubble) together with labor productivity shocks and labor supply shocks are the most important business cycle shocks. Angeletos, Collard, and Dellas (2018) argue that “confidence shocks” (which are orthogonal to fundamental shocks and arise from agents’ non-rational beliefs in the superior accuracy of their own productivity signals) are the main drivers of business cycles. In an empirical follow-up paper, Angeletos, Collard, and Dellas (2020) identify the “main business cycle shock” as a demand shock that does not strictly rely on nominal rigidity, consistent with a confidence- or sentiment-type shock.

The fact that so many different studies can reach such different conclusions about the most important business cycle shock tells us that the conclusions are likely influenced by the type of model, or the type of data, employed in the exercise. It is worth noting that none of the studies mentioned above consider U.S. asset return data measuring the equity risk premium or the bond term premium.<sup>1</sup> Moreover, none of these studies employ a model that allows for fluctuations in capital’s share of income—a distinct feature of U.S. data. Numerous authors have demonstrated that factor distribution shocks can help to explain the equity risk premium in models with concentrated capital ownership.<sup>2</sup>

In this paper, I seek to identify the main drivers of U.S. business cycles and asset returns. As noted by Campbell, Pflueger, and Viceira (2020), requiring a unified description of both macroeconomic variables and asset prices imposes valuable discipline on any model that seeks to explain the observed data. The framework for the analysis is a real business cycle model

---

<sup>1</sup>In estimating their model, Christiano, Motto, and Rostagno (2014) consider data on the value of the stock market, credit to nonfinancial firms, the credit spread of bond yields, and the term spread of bond yields. They evaluate their model using data on the cross-sectional dispersion of firm-level stock returns. In estimating their model, Miao, Wang, and Xu (2015) consider data on the value of the stock market and the Chicago Fed’s National Financial Conditions Index.

<sup>2</sup>See, for example, Danthine and Donaldson (2002), Guvenen (2009), Lansing (2015), Greenwald, Lettau, and Ludvigson (2024), and Gaudio, Petrella, and Santoro (2023).

with eight fundamental shocks and one “equity sentiment shock” that captures belief-driven fluctuations. The eight fundamental shocks influence the representative agent’s risk aversion coefficient, the disutility of labor supply, the productivity of three separate inputs that appear in the law of motion for capital, capital’s share of income, the productivity of hours worked, and the real value of coupon payments from a long-term bond.

To facilitate the replication of U.S. asset return data, the model includes an equity sentiment shock, a time-varying risk aversion coefficient (motivated by external habit formation), a shock that influences the productivity of “investor effort” in the production of new capital, and a shock that influences the real value of bond coupon payments. These four shocks allow the model to exactly replicate quarterly U.S. data for the real return on equity (including dividends) and the real returns on both short-term and long-term Treasury bonds. In so doing, the model exactly replicates quarterly U.S. data for the equity risk premium and the bond term premium.

To identify the nine model shocks (or wedges), I employ a version of the “business cycle accounting” methodology developed by Chari, Kehoe, and McGrattan (2007).<sup>3</sup> Other examples of this approach in the context of real business cycle models include Macnamara (2016), Brinca, et al. (2016), and Brinca, Costa-Filho, and Loria (2024). Šustek (2011) extends the approach to include two additional wedges that influence inflation and the short-term nominal interest rate, but these additional wedges do not affect the behavior of the model’s real variables.<sup>4</sup> In contrast to these studies, the baseline model here is designed to replicate *all* movements in the U.S. data, not just those associated with business cycle frequencies. To identify the shocks, I employ quarterly U.S. data that excludes government consumption and investment.<sup>5</sup> The sequences of the nine shocks are “reverse-engineered” so that the model exactly replicates the quarterly time paths of eleven macroeconomic variables and asset returns (only nine of which are independent). As an alternative to estimation, I calibrate the model’s parameters so that the steady state or trend values of the model variables exactly match the U.S. data in 1972:Q3—a period when key U.S. macroeconomic ratios are all close to their full-sample means.

To simplify the shock identification exercise, I assume that the boundedly-rational representative agent in the model employs univariate forecast rules for each of the nine shocks. A fully-rational agent, in contrast, would employ a nine-dimensional vector autoregression

---

<sup>3</sup>Throughout the paper, I use the term “shocks” to describe the exogenous stochastic variables that appear in the model’s equilibrium conditions.

<sup>4</sup>Similarly, the bond coupon decay shock included here does not affect the behavior of the macroeconomic variables or other asset prices.

<sup>5</sup>In a review of numerous business cycle accounting exercises in the literature, Brinca, Costa-Filho, and Loria (2024) conclude that the ability of a government consumption wedge to explain economic fluctuations “is very often either very small or nil.”

(VAR) to forecast the future shock values. Use of the VAR would imply that the agent has knowledge of the complex correlation structure among the nine shock innovations. But this correlation structure can only be observed *ex post*, after the model itself is used to identify the shocks. I show in the Appendix that the use of an *ex post* estimated VAR instead of the univariate forecast rules delivers only minor improvements in the accuracy of the shock forecasts. The univariate shock forecasts are almost perfectly correlated with the VAR shock forecasts, confirming that the univariate forecast rules are near rational.

Inclusion of the equity sentiment shock is motivated by a large literature that documents links between movements in equity prices and measures of investor or consumer sentiment.<sup>6</sup> Numerous studies find evidence of a significant empirical link between non-fundamental equity price movements and the resulting investment decisions by firms.<sup>7</sup> Recently, Bianchi, Ludvigson, and Ma (2022) and Bhandari, Borovička, and Ho (2024) present evidence that survey forecasts of economic activity and inflation exhibit persistent “belief distortions” or “belief wedges” relative to the true data generating process for the variables being forecasted. They argue that fluctuations in these objects are important drivers of the associated macroeconomic variables. The equity sentiment shock plays a similar role here.

The sentiment shock introduces a wedge between the agent’s subjective forecast of future equity value and the “fundamentals-only” forecast. This wedge can be motivated by the presence of a non-fundamental or “bubble” component of equity value. The non-fundamental equity component does not affect bond prices directly, but it does influence the agent’s consumption and thereby shift the stochastic discount factor that is used to determine the equilibrium bond prices. Due to the self-referential nature of the model and the near-unity slope of the equity market first order condition, the agent’s perception that movements in equity value are partly driven by sentiment is close to self-fulfilling. I show that the agent’s perceived law of motion for equity value delivers outcomes that are numerically very close to those generated by the actual law of motion.

The value of the model-identified sentiment shock is negative in steady state, implying that sentiment is “pessimistic” relative to fundamental equity value in 1972.Q3. This feature allows the model to replicate the equity risk premium in the data while maintaining a low level of risk aversion. Many studies show that incorporating some form of in-sample pessimistic bias about fundamentals or future equity values can magnify the equity risk premium in standard asset pricing models.<sup>8</sup> In support of this idea, Velásquez-Giraldo (2023) documents that even among

---

<sup>6</sup>See, for example, Baker and Wurgler (2007), Schmeling (2009), Greenwood and Shleifer (2014), Huang, et al. (2014), Adam, Marcet, and Beutel (2017), Frydman and Stillwagon (2018), and Lansing, LeRoy, and Ma (2022), among others.

<sup>7</sup>See, for example, Chirinko and Schaller (2001), Goyal and Yamada (2004), Gilchrist, Himmelberg, and Huberman (2005), and Campello and Graham (2013).

<sup>8</sup>See, for example, Reitz (1988), Cecchetti, Lam, and Mark (2000), Abel (2002), Cogley and Sargent (2008),

college graduates, the average respondent in the Health and Retirement Study (HRS) holds pessimistic beliefs about future equity returns relative to the historical distribution of actual returns. Bhandari, Borovička, and Ho (2024) document evidence of time-varying pessimism in survey forecasts about unemployment and inflation from the University of Michigan Survey of Consumers.

The typical business cycle accounting exercise delivers wedges that exhibit significant cross-correlations.<sup>9</sup> I find strong positive correlations between innovations to sentiment, risk aversion, and labor disutility. I also find strong positive correlations between innovations to three shocks that appear in the capital law of motion. The factor distribution shock and the labor productivity shock both appear in the aggregate production function. Innovations to these two shocks are strongly negatively correlated with each other. These patterns motivate three categories of shocks for the counterfactual scenarios: (1) only sentiment and preference shocks, (2) only capital law of motion shocks, and (3) only production function shocks. These categories roughly correspond to the three main building blocks of the model, namely, the household utility function, the law of motion for capital, and the production function for output. The counterfactual scenarios seek to identify the main source of fluctuations as roughly coming from say, household demand factors, financial factors that influence capital formation, or production/supply factors.

Brinca et al. (2016) state that business cycle accounting exercises “guide researchers to focus on the key margins that need to be distorted in order to capture the nature of the fluctuations.” Given the results, a more detailed model could then be developed to elaborate on the microfoundations that give rise to such distortions.<sup>10</sup> Looking ahead, the business cycle accounting exercise performed here finds that there is no main source of fluctuations. Rather, each of the three shock categories is important for explaining aspects of U.S. data since 1960.

As a preview of the results, the left panel of Figure 1 plots the model-identified sentiment shock together with the University of Michigan’s consumer sentiment index (which is not used in the shock identification procedure). The correlation coefficient between the two series is 0.67. The right panel of Figure 1 plots the model-identified risk aversion coefficient together with a survey-based measure of investors’ expected return on stocks over the next year, as constructed by Nagel and Xu (2022a). The correlation coefficient between the two series is 0.56. The investor expected return series is also strongly correlated with the University of Michigan’s consumer sentiment index. Similarly, the model-identified risk version coefficient is strongly correlated with the model-identified sentiment shock.

---

Barro (2009), Gourio (2012), Bidder and Dew-Becker (2016), and Adam and Merkel (2019), among others.

<sup>9</sup>Using detrended quarterly U.S. data from 1959.Q1 to 2004.Q4, Chari, Kehoe, and McGrattan (2007, p. 810) report contemporaneous cross-correlations among their four model wedges that range from  $-0.88$  to  $0.61$ .

<sup>10</sup>But as a caveat, Brinca et al. (2016) demonstrate that the “prototype model” which is used to identify the shocks/wedges may be equivalent to more than one type of detailed model.

Model risk aversion is high when the agent’s expected return on stocks is high and when stock market valuation is also high. Higher model risk aversion is achieved when agents place more emphasis on interpersonal consumption comparisons during good times. This pattern provides a partial fundamental justification for investors’ higher expected returns on stocks in good times. In contrast, models with countercyclical risk aversion deliver the exact opposite result: risk aversion and expected returns on stocks are both low in good times when stock market valuation is high (Campbell and Cochrane 1999, Cochrane 2017). Numerous studies have demonstrated that investor survey evidence strongly contradicts the predictions of models with countercyclical risk aversion.<sup>11</sup>

In the model of Campbell and Cochrane (1999), the time-varying risk aversion coefficient is constructed to be countercyclical. Here, in contrast, I use the model together with U.S. asset return data to identify a pro-cyclical risk aversion coefficient. The pro-cyclical nature of the model’s risk aversion coefficient is consistent with the findings of several empirical studies. Using a behavioral model of asset pricing, Barone-Adesi, Mancini, and Shefrin (2017) jointly estimate time-varying values for sentiment, risk aversion, and time preference using weekly data on returns and options prices for the Standard & Poor’s (S&P) 500 stock price index. The estimated risk aversion coefficient is higher after market gains and lower after market losses. Moreover, the estimated risk aversion coefficient is strongly correlated with sentiment components that measure “excessive optimism” and “overconfidence.” Using monthly data on options for the S&P 500 index, Kosolapova, Hanke and Weissensteiner (2023) estimate a time-varying risk aversion coefficient for the marginal investor that is strongly pro-cyclical. Their study builds on earlier work by Bliss and Panigirtzoglou (2004) who find that risk aversion is lower during sample periods with high stock market volatility, such as crises. They postulate that one explanation for this result is that the representative investor changes as market volatility changes. This could occur if high risk-averse investors leave the equity market during downturns or periods of high volatility, resulting in a lower average level of risk aversion among investors who remain in the market.

Cochrane (2017, p. 966) observes: “There is no way to tell risk aversion—marginal utility—from a probability distortion...without some restriction—some model that ties either probability distortions or marginal utility to observables.” Along these lines, the model-identified risk aversion coefficient represents marginal utility while the model-identified sentiment shock represents a probability distortion. Given the model and the other seven shock sequences, the reverse-engineering exercise tells us how to separate marginal utility (risk aversion) from a probability distortion (sentiment) in order to exactly replicate the U.S. data.

---

<sup>11</sup>See, for example, Vissing-Jørgensen (2004), Amromin and Sharpe (2014), Greenwood and Shleifer (2014), Adam, Marcet, Beutel (2017), Giglio, et al. (2021), Adam, Matveev, and Nagel (2021), and Nagel and Xu (2022b).

Using impulse response functions, I show that each of the three main shock categories noted above can generate all or most of the features of a typical business cycle. For example, higher sentiment together with higher risk aversion delivers a correlated increase in all macroeconomic variables. Equity value increases but bond prices decline, implying an increase in bond yields. The combination of these two highly correlated shocks delivers the features observed during a typical economic boom or recovery. A positive innovation to capital’s share of income in the production function delivers a very similar response pattern except that hours worked now undergoes a small decline. Higher values for the capital law of motion shocks also deliver a correlated increase in macroeconomic variables. Equity value declines on impact (with bond prices) but then rises with investment. These results show that many key features of U.S. business cycles can arise from a variety of sources within the model.<sup>12</sup>

Given the model-identified shock sequences, I perform the typical business cycle accounting exercises that involve counterfactual scenarios. Each scenario adds one category of shock realizations while other shocks are set equal to steady state or trend values. To gauge the importance of each shock category, I compute various summary statistics. For fluctuations at business cycle frequencies, I compute the correlation coefficient between a detrended model variable under a given shock scenario and the detrended U.S. variable. To gauge the importance of each shock category for lower frequency movements, I first compute the squared percentage gaps between the counterfactual model paths and the U.S. data paths for each variable, without any detrending. A smaller gap measure implies that a given shock scenario does a better job of explaining total movements in the U.S. variable. Following Brinca, et al. (2016), and Brinca, Costa-Filho, and Loria (2024), I then normalize the cumulative squared gaps across shock scenarios to construct an index that measures fraction of total movements in each variable that can be explained by each shock scenario.

The correlation coefficients between the model and the U.S. data show that each of the three main shock categories is the most important driver of at least one macroeconomic variable or asset price. For example, the sentiment and preference shocks are the most important drivers of business cycle movements in output, investment, hours worked, and the price of the short-term bond (which determines the risk free rate of return). Recall that this category of shocks includes the time-varying risk aversion coefficient and the labor disutility shock. The capital law of motion shocks are the most important drivers of business cycle movements in the capital stock and equity value. The production function shocks are the most important drivers of business cycle movements in consumption. But none of the three main shock categories can account for movements in the price of the long-term bond. Rather, this asset

---

<sup>12</sup>Along similar lines, Gaudio, Petrella, and Santoro (2023) show that correlated increases in macroeconomic variables can arise from three different (but correlated) shocks that either appear in the production function or influence capital accumulation.

price is driven mainly by the highly-specific coupon decay shock. This last result tell us that movements in the long-term bond price cannot be readily explained by shocks that account for movements in equity value or the short-term bond price.

Another important result is that each of the three counterfactual shock scenarios can account for a sizeable fraction of both business cycle movements and total movements in most U.S. variables. For example, the correlation coefficients between detrended model output and detrended U.S. output range from 0.40 to 0.69 across the three shock scenarios. For total movements, no single shock category is clearly dominant for many of the variables, including output. While some variables are driven by a single dominant shock category, the dominant category is different for each of those variables. Taken as a whole, the results tell us that each of the three main shock categories is important for explaining U.S. data since 1960.

Finally, I assess how each shock scenario performs in explaining the Great Recession (2007.Q4 to 2009.Q2) versus the Covid recession (2019.Q4 to 2020.Q2). Starting from 2007.Q4, I add one category of shock realizations while other shocks are set equal to steady state or trend values. According to the model, the decline in U.S. output during the Great Recession was driven mainly by capital law of motion shocks together with sentiment and preference shocks. This is consistent with the idea that both financial and demand factors played a significant role during the Great Recession. According to the model, the decline in U.S. output during the Covid recession was driven mainly by sentiment and preference shocks together with production function shocks. This is consistent with idea that both demand and supply factors played a significant role in the Covid recession. Overall, the results tell us that U.S. recessions have been driven by different types of shocks.

Some may wonder whether the finding that there is no “most important shock” is robust to the use of a broader framework or a richer model. The answer can be found in the results of the many previous studies that have already employed broader frameworks and richer models, as reviewed above in the first paragraph of the introduction. Despite the additional model complexities and the use of novel data or methods, each previous study reaches a different conclusion about the most important shock. The application of Occam’s razor suggests that the simplest explanation for the disagreement across studies is that there is no most important shock to be found.

In discussing the identification of a “main business cycle shock,” Angeletos, Collard, and Dellas (2020, p. 3054) acknowledge “In principle, any of the reduced-form objects contained in our anatomy may map into a uninterpretable combination of multiple theoretical shocks, none of which possesses the properties of the empirical object.” The results presented here show that a complex combination of multiple theoretical shocks is indeed necessary to fully explain the historical patterns of U.S. business cycles and asset returns. Finding a simpler explanation for the historical patterns is likely to prove extremely difficult.

**Additional related literature.** The model-identified shocks are Solow-type residuals that act as stand-ins for whatever time-varying model complexities are needed to replicate the U.S. data. Cúrdia and Reis (2011), Andrieu (2014), and Andrieu, Brûha, and Solmaz (2017) argue that the cross-correlation pattern of the identified shocks can provide useful information about what may be needed to improve the model’s fit via endogenous mechanisms. Falter and Wesselbaum (2018) examine the impact of correlated shocks in the context of three benchmark macro models developed by Bernanke, Gertler, and Gilchrist (1999), Iacoviello (2005), and Justiniano, Primiceri, and Tambalotti (2010). In each case, the model with correlated shocks matches the data much better than the version with uncorrelated shocks. Gaudio, Petrella, and Santoro (2023) consider a concentrated capital ownership model with three exogenous shocks: A neutral technology shock (analogous to the labor productivity shock here), an investment specific technology shock (analogous to a capital law of motion shock here), and a factor share shock (analogous to the factor distribution shock here). The model allows for cross-correlation among the three shock innovations, as governed by an estimated VAR. A study by Morely, Nelson, and Zivot (2003) documents a significant negative correlation between innovations to the trend versus cycle components of U.S. GDP, in contrast to the orthogonal assumption embedded in most unobserved-component time series models. For models with multiple shocks and occasionally binding constraints, Ascari and Mavroeidis (2022) demonstrate that the existence of equilibrium requires interdependent restrictions on the support of the various shocks. This “coherency condition” is not compatible with the assumption of orthogonal shocks.

**Layout.** The remainder of this paper is organized as follows. Section 2 describes the model and the manner in which I introduce equity sentiment. Section 3 describes the identification of parameter values and the sequences of shock realizations so that the model exactly replicates quarterly U.S. data from 1960.Q1 to 2022.Q4. Section 4 presents quantitative exercises, including counterfactual shock scenarios. Section 5 concludes. The appendix provides details of the model solution, the shock identification procedure, data sources and methods, and an analysis of the representative agent’s forecast accuracy.

## 2 Model

The framework for the analysis is a real business cycle model that includes eight fundamental shocks and one equity sentiment shock that captures belief-driven fluctuations. The representative agent’s decision problem is to maximize

$$\tilde{E}_0 \sum_{t=0}^{\infty} \beta^t \left[ \log(c_t - \kappa_t C_t) - D \exp(u_t) \frac{(h_{1,t} + h_{2,t})^{1+\gamma}}{1 + \gamma} \right], \quad (1)$$

subject to the budget constraint

$$c_t + i_t = w_t h_{1,t} + r_t k_t, \quad (2)$$

where  $c_t$  is real consumption,  $h_{1,t}$  is hours worked in the production of output,  $h_{2,t}$  is hours worked in the production of new capital (called investor effort),  $i_t$  is investment,  $w_t$  is the real wage per hour,  $r_t$  is the real rental rate per unit of capital, and  $k_t$  is the stock of real physical capital. All quantities are measured in per person terms. The parameter  $\beta > 0$  is the agent's subjective time discount factor.

The symbol  $\tilde{E}_t$  represents the agent's subjective expectation, conditional on information available at time  $t$ . Under fully-rational expectations,  $\tilde{E}_t = E_t$ , where  $E_t$  corresponds to the mathematical expectation operator evaluated using the objective distribution of all shocks, which are assumed known to a fully-rational agent. I will also employ a "model-consistent" expectation operator  $E_t^m$  that delivers forecasts consistent with the actual laws of motion of the relevant objects in the theoretical model which presumes orthogonal shocks. But as we shall see, the model-identified shocks from U.S. data are not orthogonal. Hence,  $E_t^m$  must be viewed as boundedly-rational in the context of the U.S. data that the model seeks to replicate.

To allow for time-varying risk aversion, I assume that the representative agent derives utility from individual consumption  $c_t$  measured relative to a reference level that depends on the amount of aggregate consumption per person  $C_t$ , which is viewed by the agent as exogenous.<sup>13</sup> The reference level of consumption is often defined in terms of  $C_{t-1}$  or  $c_{t-1}$  as opposed to  $C_t$ .<sup>14</sup> But in the continuous-time limit, there is no distinction between the values of  $C_t$  and  $C_{t-1}$ . Defining the reference level in terms of  $C_t$  reduces the number of endogenous state variables and simplifies the equilibrium solution of the model without significantly influencing the model-identified shocks.

The time-varying parameter  $\kappa_t$  determines the agent's subjective coefficient of relative risk aversion  $\eta_t$  according to the relationship

$$\begin{aligned} \eta_t &\equiv -c_t \frac{U_{cc}(c_t, C_t)}{U_c(c_t, C_t)}, \\ &= -c_t \frac{-1/(c_t - \kappa_t C_t)^2}{1/(c_t - \kappa_t C_t)} = \frac{1}{1 - \kappa_t}, \end{aligned} \quad (3)$$

where I have imposed the equilibrium condition  $c_t = C_t$  in the second line of the expression.<sup>15</sup> The agent's time-varying risk aversion coefficient evolves according to the following stationary

---

<sup>13</sup>Maurer and Meier (2008) find strong empirical evidence for *contemporaneous* "peer-group effects" on individual consumption decisions using panel data on U.S. household expenditures.

<sup>14</sup>See, for example, Otrok, Ravikumar and Whiteman (2002), Beaubrun-Diant and Tripier (2005), Christiano, Motto, and Rostagno (2014), and Lansing (2015).

<sup>15</sup>If the reference level of consumption is instead defined in terms of  $C_{t-1}$ , then the subjective risk aversion coefficient is given by  $\eta_t = 1/(1 - \kappa_t/g_t^c)$ , where  $g_t^c \equiv c_t/c_{t-1}$  is the gross growth rate of real consumption per person.

law of motion

$$\eta_t = \eta_{t-1}^{\rho_\eta} \bar{\eta}^{1-\rho_\eta} \exp(\varepsilon_{\eta,t}), \quad |\rho_\eta| < 1, \quad \varepsilon_{\eta,t} \sim NID(0, \sigma_{\varepsilon,\eta}^2), \quad (4)$$

which ensures  $\eta_t > 0$ . The parameter  $\rho_\eta$  governs the persistence of the risk aversion coefficient and  $\varepsilon_{\eta,t}$  is a normally and independently distributed (*NID*) innovation with mean zero and variance  $\sigma_{\varepsilon,\eta}^2$ . The steady state level of risk aversion is given by  $\bar{\eta}$ . For the quantitative analysis, I will employ  $\bar{\eta} = 1$  such that  $\bar{\kappa} = 0$ .<sup>16</sup>

The agent supplies labor to productive firms in the amount  $h_{1,t}$ . Following Zhu (1995), the agent also supplies “investor effort” in the amount  $h_{2,t}$  that contributes to the production of new capital, as described further below. The disutility of total labor supplied is governed by the second term in (1), where  $D > 0$ , and  $\gamma \geq 0$ . The Frisch elasticity of labor supply is given by  $1/\gamma$ . As  $\gamma \rightarrow \infty$ , the model reduces to one with fixed labor supply. Following Hall (1997), I allow for a “labor disutility shock”  $u_t$  (also called a labor supply shock in the literature) that shifts the intratemporal trade-off between consumption and leisure. In support of this idea, Kaplan and Schulhofer-Wohl (2018) find that labor disutility, as measured by “feelings about work” from surveys, has shifted in significant ways since 1950. More generally, the shock  $u_t$  could also be interpreted as a “labor wedge” that captures fluctuations in the effective tax rate on labor income. The labor disutility shock evolves according to the following stationary AR(1) process.

$$u_t = \rho_u u_{t-1} + \varepsilon_{u,t}, \quad |\rho_u| < 1, \quad \varepsilon_{u,t} \sim NID(0, \sigma_{\varepsilon,u}^2). \quad (5)$$

The representative agent derives income by supplying labor and capital services to identical competitive firms. Firms produce output according to the technology

$$y_t = A k_t^{\alpha_t} [\exp(z_t) h_{1,t}]^{1-\alpha_t}, \quad A > 0, \quad (6)$$

$$z_t = z_{t-1} + \mu + \varepsilon_{z,t}, \quad \varepsilon_{z,t} \sim NID(0, \sigma_{\varepsilon,z}^2), \quad (7)$$

$$\alpha_t = \alpha_{t-1}^{\rho_\alpha} \bar{\alpha}^{1-\rho_\alpha} \exp(\varepsilon_{\alpha,t}), \quad |\rho_\alpha| < 1, \quad \varepsilon_{\alpha,t} \sim NID(0, \sigma_{\varepsilon,\alpha}^2). \quad (8)$$

In equation (6),  $z_t$  represents a “labor productivity shock” that evolves as a random walk with drift. The drift parameter  $\mu > 0$  determines the trend growth rate of output per person in the economy. Stochastic variation in the production function exponent  $\alpha_t$  represents a “factor distribution shock,” along the lines of Young (2004), Ríos-Rull and Santaepulàlia-Llopis (2010), Lansing (2015), and Lansing and Markiewicz (2018). The logarithm of  $\alpha_t$  evolves as a stationary AR(1) process.

---

<sup>16</sup>Greenwald, Lettau, and Ludvigson (2024) develop a related model where the risk aversion coefficient and the risk free rate of return are each governed by an exogenous stochastic process.

Profit maximization by firms yields the factor prices

$$w_t = (1 - \alpha_t) y_t / h_{1,t}, \quad (9)$$

$$r_t = \alpha_t y_t / k_t, \quad (10)$$

which together imply  $y_t = w_t h_{1,t} + r_t k_t$ . From equation (10), stochastic variation in  $\alpha_t$  allows the model to replicate fluctuations in the U.S. capital share of income, as represented by  $r_t k_t / y_t$ . Given the time series for  $\alpha_t$ , stochastic variation in  $z_t$  allows equation (6) to replicate fluctuations in U.S. output.

Resources devoted to investment together with investor effort contribute to the production of new capital according to the following law of motion

$$k_{t+1} = B \exp(v_t) k_t^{1-\delta_t-\varphi_t} i_t^{\delta_t} [\exp(z_t) h_{2,t}]^{\varphi_t}, \quad B > 0, \quad (11)$$

$$v_t = \rho_v v_{t-1} + \varepsilon_{v,t}, \quad |\rho_v| < 1, \quad \varepsilon_{v,t} \sim NID(0, \sigma_{\varepsilon,v}^2), \quad (12)$$

$$\delta_t = \delta_{t-1}^{\rho_\delta} \bar{\delta}^{1-\rho_\delta} \exp(\varepsilon_{\delta,t}), \quad |\rho_\delta| < 1, \quad \varepsilon_{\delta,t} \sim NID(0, \sigma_{\varepsilon,\delta}^2), \quad (13)$$

$$\varphi_t = \varphi_{t-1}^{\rho_\varphi} \bar{\varphi}^{1-\rho_\varphi} \exp(\varepsilon_{\varphi,t}), \quad |\rho_\varphi| < 1, \quad \varepsilon_{\varphi,t} \sim NID(0, \sigma_{\varepsilon,\varphi}^2), \quad (14)$$

where the shocks  $v_t$ ,  $\delta_t$ , and  $\varphi_t$  can be interpreted as capturing financial factors that impact the supply of new capital and the price of claims to existing capital. A study by Greenwood, Hercowitz, and Huffman (1988) was the first to demonstrate that shocks of this sort can be an important driving force for business cycle fluctuations.<sup>17</sup> The log-linear formulation of equation (11) captures the presence of capital adjustment costs.<sup>18</sup>

Following Lansing and Markiewicz (2018), I allow for a “multiplier shock”  $v_t$  that evolves as a stationary AR(1) process. Stochastic variation in  $v_t$  allows equation (11) to replicate the time path of U.S. private nonresidential fixed assets. The variable  $\delta_t$  is an “investment shock” that represents stochastic variation in the elasticity of new capital with respect to investment. The variable  $\varphi_t$  is an “investor effort shock” that represents stochastic variation in the elasticity of new capital with respect to investor effort. Analogous to equation (6), the productivity of investor effort is influenced by the labor productivity shock  $z_t$ . The logarithms of  $\delta_t$  and  $\varphi_t$  evolve as stationary AR(1) processes.

<sup>17</sup>Other examples along these lines include Ambler and Paquet (1994), Justiniano, Primiceri, and Tambalotti (2010), Liu, Waggoner, and Zha (2011), and Furlanetto and Seneca (2014).

<sup>18</sup>When  $\delta_t < 1$ , one unit of new investment produces less than one unit of new capital. Lansing (2012) shows that equation (11) with  $\varphi_t = 0$  maps directly to a log-linear approximate version of the law of motion for capital employed by Jermann (1998).

The agent's first-order conditions with respect to  $c_t$ ,  $h_{1,t}$ ,  $h_{2,t}$ , and  $k_{t+1}$  are given by

$$\lambda_t = 1/(c_t - \kappa_t C_t) = \eta_t/c_t, \quad (15)$$

$$D \exp(u_t) (h_{1,t} + h_{2,t})^\gamma = \lambda_t w_t, \quad (16)$$

$$D \exp(u_t) (h_{1,t} + h_{2,t})^\gamma = \lambda_t \varphi_t i_t / (\delta_t h_{2,t}), \quad (17)$$

$$\lambda_t i_t / (\delta_t k_{t+1}) = \beta \tilde{E}_t \lambda_{t+1} [r_{t+1} + (1 - \delta_{t+1} - \varphi_{t+1}) i_{t+1} / (\delta_{t+1} k_{t+1})], \quad (18)$$

where  $\lambda_t$  is the Lagrange multiplier on the budget constraint (2). In equation (15), I have imposed the equilibrium relationships  $c_t = C_t$  and  $\eta_t = 1/(1 - \kappa_t)$ . In deriving equation (18), I start by using the capital law of motion (11) to eliminate  $i_t$  from the budget constraint (2).

Combining equations (9), (16), and (17) yields the following expression for total hours worked  $h_t$ :

$$\underbrace{h_{1,t} + h_{2,t}}_{h_t} = \left\{ \frac{\eta_t}{D \exp(u_t)} \left[ (1 - \alpha_t) \frac{y_t}{c_t} + \frac{\varphi_t i_t}{\delta_t c_t} \right] \right\}^{1/(1+\gamma)}. \quad (19)$$

Given the time series for the shocks  $\alpha_t$ ,  $\eta_t$ ,  $\delta_t$ , and  $\varphi_t$ , stochastic variation in  $u_t$  allows equation (19) to replicate the time path of U.S. hours worked per person.

Since  $k_{t+1}$  is known at time  $t$ , equation (18) can be rewritten as follows

$$\underbrace{i_t/\delta_t}_{p_{s,t}} = \tilde{E}_t \left\{ M_{t+1} \underbrace{[\alpha_{t+1} y_{t+1} - (1 + \varphi_{t+1}/\delta_{t+1}) i_{t+1}]_{d_{t+1}}} + \underbrace{i_{t+1}/\delta_{t+1}}_{p_{s,t+1}} \right\}, \quad (20)$$

where  $M_{t+1} \equiv \beta (\eta_{t+1}/\eta_t) (c_{t+1}/c_t)^{-1}$  is the equilibrium stochastic discount factor. The steady state stochastic discount factor, given by  $\bar{M} \equiv \beta \exp(-\mu)$ , does not depend on the steady state value  $\bar{\eta}$ .

The rewritten first-order condition (20) is in the form of a standard asset pricing equation where  $p_{s,t} = i_t/\delta_t$  is the market value of the agent's equity shares in the firm. Equity shares are assumed to exist in unit net supply and entitle the agent to a perpetual stream of dividends starting in period  $t + 1$ . From equations (16) and (17), we have  $\varphi_t i_t/\delta_t = w_t h_{2,t}$ . Dividends in period  $t$  can therefore be written as

$$d_t = \alpha_t y_t - i_t - w_t h_{2,t}, \quad (21)$$

which shows that the shadow wage bill for investor effort subtracts from the residual cash flow that can be paid out as dividends.

Stochastic variation in  $\delta_t$  allows the model to replicate fluctuations in U.S. investment conditional on U.S. equity value. Stochastic variation in  $\varphi_t$  allows the model to replicate fluctuations in U.S. dividends. Stochastic variation in an "equity sentiment shock"  $s_t$  (introduced below) allows  $p_{s,t}$  in the model to replicate fluctuations in the real market value

of the S&P 500 stock price index. In so doing, the model's real equity return, given by  $r_{s,t} = (p_{s,t} + d_t)/p_{s,t-1} - 1$ , replicates the real return on the S&P 500 stock index.

In addition to equity shares, the representative agent can purchase default free bonds that exist in zero net-supply. One-period discount bonds purchased at the price  $p_{b,t}$  yield a single payoff of one consumption unit per bond in period  $t + 1$ . Long-term bonds (consols) purchased at the ex-coupon price  $p_{c,t}$  yield a perpetual stream of stochastically-decaying coupon payments (measured in consumption units) starting in period  $t + 1$ . The equilibrium prices of the bonds are determined by the following first-order conditions

$$p_{b,t} = E_t^m M_{t+1}, \quad (22)$$

$$p_{c,t} = E_t^m M_{t+1} [1 + \bar{\delta}_c \exp(\omega_{t+1}) p_{c,t+1}], \quad (23)$$

where  $E_t^m$  implies that the agent's bond market forecasts are consistent with the actual laws of motion of the relevant objects in the theoretical model. Consequently, departures from model-consistent expectations are restricted to the equity market and these departures turn out to be very small. The variable  $\delta_{c,t+1} \equiv \bar{\delta}_c \exp(\omega_{t+1})$  is the stochastic decay rate of the coupon received in period  $t + 1$ . The parameter  $\bar{\delta}_c \in [0, 1)$  is the steady state decay rate which influences the Macaulay duration of the bond, i.e., the present-value weighted average maturity of the bond's cash flows.<sup>19</sup> The shock  $\omega_t$  captures stochastic variation in the real value of the bond coupon payment (for example, due to surprise inflation) and evolves according to the following stationary AR(1) process

$$\omega_t = \rho_\omega \omega_{t-1} + \varepsilon_{\omega,t}, \quad |\rho_\omega| < 1, \quad \varepsilon_{\omega,t} \sim NID(0, \sigma_{\varepsilon,\omega}^2).$$

The model solutions for  $p_{b,t}$  and  $p_{c,t}$  are used to identify the sequences for the shocks  $\eta_t$  and  $\omega_t$ . The risk free rate of return is given by  $r_{b,t+1} = 1/p_{b,t} - 1$ , which is known at time  $t$ . Fluctuations in  $\eta_t$  influence  $M_{t+1}$  and thereby allow the model to replicate the real return on a 3-month U.S. Treasury bill. The risky return on the long-term bond is given by  $r_{c,t+1} = [1 + \bar{\delta}_c \exp(\omega_{t+1}) p_{c,t+1}]/p_{c,t} - 1$ . Given the model-implied sequence for  $M_{t+1}$ , fluctuations in  $\omega_t$  allow the model to replicate the real return on a long-term U.S. Treasury bond.

---

<sup>19</sup>The stochastic stream of coupon payments is given by:  $1, \bar{\delta}_c \exp(\omega_{t+1}), \bar{\delta}_c^2 \exp(\omega_{t+1} + \omega_{t+2}), \bar{\delta}_c^3 \exp(\omega_{t+1} + \omega_{t+2} + \omega_{t+3}) \dots$

## 2.1 Fundamental equity value

Defining the risk adjusted equity value-consumption ratio (a stationary variable) as  $x_t \equiv \eta_t p_{s,t}/c_t = \eta_t i_t/(\delta_t c_t)$ , the intertemporal first order condition (20) can be rewritten as follows

$$\begin{aligned} \underbrace{x_t}_{\eta_t p_{s,t}/c_t} &= \beta \tilde{E}_t \{ \eta_{t+1} \alpha_{t+1} y_{t+1}/c_{t+1} + (1 - \delta_{t+1} - \varphi_{t+1}) x_{t+1} \} \\ &= \beta \tilde{E}_t \{ \underbrace{\eta_{t+1} \alpha_{t+1} + [1 - \delta_{t+1} (1 - \alpha_{t+1}) - \varphi_{t+1}]}_{q_{t+1}} x_{t+1} \}, \end{aligned} \quad (24)$$

where I have substituted in for  $M_{t+1}$  and collected terms dated  $t$  on the left side. In the second line, I use the budget constraint (2) at time  $t + 1$  and the definition of  $x_{t+1}$  to make the substitution  $y_{t+1}/c_{t+1} = 1 + \delta_{t+1} x_{t+1}/\eta_{t+1}$ .

At this point, it is convenient to define a nonlinear change of variables such that  $q_{t+1}$  represents the composite stationary variable that the agent must forecast.<sup>20</sup> The agent's first-order condition (24) becomes  $x_t = \beta \tilde{E}_t q_{t+1}$ . Now using the definition of  $q_t$  to make the substitution  $x_t = (q_t - \alpha_t \eta_t) / [1 - \delta_t (1 - \alpha_t) - \varphi_t]$  in equation (24) yields the following transformed version of the agent's first order condition

$$q_t = \eta_t \alpha_t + [1 - \delta_t (1 - \alpha_t) - \varphi_t] \beta \tilde{E}_t q_{t+1}. \quad (25)$$

The fundamental equity value  $q_t^f$  is obtained by solving equation (25) under the assumption of model-consistent expectations such that  $\tilde{E}_t q_{t+1}^f = E_t^m q_{t+1}^f$ . As shown in Appendix A, a log-linear approximate version of the fundamental solution is given by

$$q_t^f = \bar{q}^f \left[ \frac{\eta_t}{\bar{\eta}} \right]^{\gamma_\eta} \left[ \frac{\alpha_t}{\bar{\alpha}} \right]^{\gamma_\alpha} \left[ \frac{\delta_t}{\bar{\delta}} \right]^{\gamma_\delta} \left[ \frac{\varphi_t}{\bar{\varphi}} \right]^{\gamma_\varphi}, \quad (26)$$

where  $\bar{q}^f \equiv \exp[E_t^m \log(q_t^f)]$  and  $\gamma_\eta$ ,  $\gamma_\alpha$ ,  $\gamma_\delta$ , and  $\gamma_\varphi$  are solution coefficients that depend on model parameters and shock variances. Given the value of  $q_t^f$ , we can recover the fundamental equity value-consumption ratio as

$$\frac{p_{s,t}^f}{c_t} = \frac{(q_t^f - \alpha_t)/\eta_t}{1 - \delta_t (1 - \alpha_t) - \varphi_t}, \quad (27)$$

which shows that  $p_{s,t}^f/c_t$  will only move in response to the four fundamental shocks  $\eta_t$ ,  $\alpha_t$ ,  $\delta_t$ , and  $\varphi_t$ . Two of these shocks,  $\delta_t$  and  $\varphi_t$ , appear in the law of motion for capital,  $\eta_t$  appears in the utility function, and  $\alpha_t$  appears in the production function. Notably, the labor productivity shock  $z_t$  has no influence on this equity valuation ratio.

<sup>20</sup>This nonlinear change of variables technique and the associated solution method is also employed in Lansing (2010, 2016) and Lansing and LeRoy (2014).

## 2.2 Introducing equity sentiment

Pigou (1927, p.73) attributed business cycle fluctuations partly to “psychological causes” which lead people to make “errors of undue optimism or undue pessimism in their business forecasts.” Keynes (1936, p.156) likened the stock market to a “beauty contest” where participants devote their efforts not to judging the underlying concept of beauty, but instead to “anticipating what average opinion expects the average opinion to be.” Numerous empirical studies starting with Shiller (1981) and LeRoy and Porter (1981) have shown that equity prices appear to exhibit excess volatility when compared to fundamentals, as measured by the discounted stream of ex post realized dividends.<sup>21</sup> Kocherlakota (2010) remarks: “I believe that [macroeconomists] are handicapping themselves by only looking at shocks to fundamentals like preferences and technology. Phenomena like credit market crunches or asset market bubbles rely on self-fulfilling beliefs about what others will do.”<sup>22</sup> Recent empirical studies by Bianchi, Ludvigson, and Ma (2022) and Bhandari, Borovička, and Ho (2024) find that “belief distortions” or “belief wedges” are important drivers of key macroeconomic variables.

To capture the flavor of the above ideas, I postulate that the representative agent’s perceived law of motion (PLM) for the composite variable  $q_t$  allows for the possibility of departures from the fundamental value  $q_t^f$ . Specifically, the agent’s PLM takes the form

$$q_t = \exp(s_t) q_t^f, \quad (28)$$

$$s_t = \bar{s} + \rho_s(s_{t-1} - \bar{s}) + \varepsilon_{s,t}, \quad |\rho_s| < 1, \quad \varepsilon_{s,t} \sim NID(0, \sigma_{\varepsilon,s}^2), \quad (29)$$

where the sentiment shock  $s_t$  evolves as a stationary AR(1) process. The PLM predicts that  $q_t/q_t^f$  is increasing in  $s_t$ , where  $q_t$  is the actual value observed in the data and  $q_t^f$  is the value predicted by fundamentals from equation (26).<sup>23</sup>

The form of the PLM (28) can be motivated by the perception of a non-fundamental or “bubble” component of equity value, denoted by  $q_t^b$ . Substituting  $q_t = q_t^f + q_t^b$  into equation (28) yields the following perceived law of motion for the non-fundamental component of equity value

$$q_t^b = [\exp(s_t) - 1] q_t^f. \quad (30)$$

Unlike a rational bubble, equation (30) allows for the possibility of  $q_t^b < 0$  when  $s_t < 0$ . Equation (30) implies that fluctuations in  $s_t$  generate movements in  $q_t^b$  that, in turn, influence movements in  $q_t = q_t^f + q_t^b$ .<sup>24</sup> In equilibrium, the agent’s perception that movements in  $q_t$

---

<sup>21</sup>Lansing and LeRoy (2014) provide an update on this literature.

<sup>22</sup>There are a variety of ways in which sentiment or animal spirits-type mechanisms can be incorporated into quantitative business cycle models. For a brief review, see Lansing (2019).

<sup>23</sup>Yu (2013) introduces a persistent sentiment shock that acts as a wedge between the actual versus perceived laws of motion for consumption growth in an endowment economy.

<sup>24</sup>Lansing (2012) examines a bubble component of equity value that is driven by fluctuations in fundamental technology shocks.

are partly driven by sentiment is close to self-fulfilling. The value of  $q_t^b$  does not affect bond prices directly, but it does influence the agent's consumption and thereby shift the stochastic discount factor  $M_{t+1}$  that is used to determine the equilibrium bond prices.

Given the PLM (28), the agent's subjective forecast for next period's equity value can be computed as follows

$$\begin{aligned}
\tilde{E}_t q_{t+1} &= \exp[\bar{s} + \rho_s(s_t - \bar{s}) + \sigma_{\varepsilon,s}^2/2] E_t^m q_{t+1}^f, \\
&= \underbrace{\exp(\bar{s} + \sigma_{\varepsilon,s}^2/2 + \gamma_\eta^2 \sigma_{\varepsilon,\eta}^2/2 + \gamma_\alpha^2 \sigma_{\varepsilon,\alpha}^2/2 + \gamma_\delta^2 \sigma_{\varepsilon,\delta}^2/2 + \gamma_\varphi^2 \sigma_{\varepsilon,\varphi}^2/2)}_{\bar{q}} \bar{q}^f \\
&\quad \times \exp[\rho_s(s_t - \bar{s})] \left[ \frac{\eta_t}{\bar{\eta}} \right]^{\rho_\eta \gamma_\eta} \left[ \frac{\alpha_t}{\bar{\alpha}} \right]^{\rho_\alpha \gamma_\alpha} \left[ \frac{\delta_t}{\bar{\delta}} \right]^{\rho_\delta \gamma_\delta} \left[ \frac{\varphi_t}{\bar{\varphi}} \right]^{\rho_\varphi \gamma_\varphi}, \tag{31}
\end{aligned}$$

where  $E_t^m q_{t+1}^f$  is the model-consistent “fundamentals-only” forecast that is computed from the fundamental solution (26). The term  $\exp[\bar{s} + \rho_s(s_t - \bar{s}) + \sigma_{\varepsilon,s}^2/2]$  in equation (31) acts as a wedge between the agent's subjective forecast and the fundamentals-only forecast. The basic structure of equation (31) is consistent with the empirical results of Frydman and Stillwagon (2018) who find that investors' expectations about future stock returns from surveys are driven by both fundamental and behavioral factors.

Substituting the agent's subjective forecast (31) into the transformed first order condition (25) yields the actual law of motion (ALM) for  $q_t$ . The first order condition is “self-referential,” meaning that the actual value of  $q_t$  depends in part on the agent's subjective forecast  $\tilde{E}_t q_{t+1}$ . From the perspective of any individual agent, switching to the fundamentals-only forecast would appear to reduce forecast accuracy, so there is no incentive to switch.<sup>25</sup> When the intercept term  $\eta_t \alpha_t$  in equation (25) is close to zero, the first order condition approximates a no-arbitrage bubble condition for which there may exist a continuum of self-fulfilling solutions.<sup>26</sup> But even when  $\eta_t \alpha_t > 0$ , the actual value of  $q_t$  can closely approximate the value predicted by the PLM (28) if the slope coefficient  $[1 - \delta_t(1 - \alpha_t) - \varphi_t] \beta$  that multiplies  $\tilde{E}_t q_{t+1}$  is close to 1.0. I will show that this near-unity property of the slope coefficient is satisfied in the quantitative version of the model. Consequently, the agent's perception that movements in equity value are partly driven by sentiment is close to self-fulfilling. The near-unity slope of equation (25) implies that the value of  $q_t^b$  from equation (30) approximately satisfies the following no-arbitrage condition

$$q_t^b = [1 - \delta_t(1 - \alpha_t) - \varphi_t] \beta \tilde{E}_t q_{t+1}^b. \tag{32}$$

<sup>25</sup>Lansing (2006) explores the concept of “forecast lock-in” using a simple asset pricing model with extrapolative expectations.

<sup>26</sup>Lansing (2010) provides examples of rational bubble solutions in an endowment economy.

Given the realized value of  $q_t$ , we can recover the equity value-consumption ratio as

$$\frac{p_{s,t}}{c_t} = \frac{(q_t - \alpha_t)/\eta_t}{1 - \delta_t(1 - \alpha_t) - \varphi_t}, \quad (33)$$

where  $q_t = q(\eta_t, \alpha_t, \delta_t, \varphi_t, s_t)$ . Hence in equilibrium,  $p_{s,t}/c_t$  will be partly driven by sentiment because the agent's subjective forecast (31) makes use of the sentiment variable. Using equation (33), we can recover the risk adjusted equity value-consumption ratio as

$$x_t \equiv \frac{\eta_t p_{s,t}}{c_t} = \frac{\eta_t \dot{i}_t}{\delta_t c_t} = \frac{q_t - \alpha_t}{1 - \delta_t(1 - \alpha_t) - \varphi_t}, \quad (34)$$

where  $x_t = x(\eta_t, \alpha_t, \delta_t, \varphi_t, s_t)$ . Alternatively, since  $x_t = \beta \tilde{E}_t q_{t+1}$ , we can recover  $x_t$  by multiplying the agent's subjective forecast (31) by  $\beta$ .

### 2.3 Equilibrium macroeconomic variables and asset returns

Given the equilibrium value of  $x_t$  from equation (34), the equilibrium values of the other macroeconomic variables can be computed using the following equations

$$h_t = \{D^{-1} \exp(-u_t) [(1 - \alpha_t)(\eta_t + \delta_t x_t) + \varphi_t x_t]\}^{1/(1+\gamma)}, \quad (35)$$

$$h_{1,t} = \{[(1 - \alpha_t)(\eta_t + \delta_t x_t)] / [(1 - \alpha_t)(\eta_t + \delta_t x_t) + \varphi_t x_t]\} h_t, \quad (36)$$

$$h_{2,t} = \{\varphi_t x_t / [(1 - \alpha_t)(\eta_t + \delta_t x_t) + \varphi_t x_t]\} h_t, \quad (37)$$

$$y_t = A k_t^{\alpha_t} [\exp(z_t) h_{1,t}]^{1-\alpha_t}, \quad (38)$$

$$c_t = [\eta_t / (\eta_t + \delta_t x_t)] y_t, \quad (39)$$

$$i_t = [\delta_t x_t / (\eta_t + \delta_t x_t)] y_t, \quad (40)$$

$$p_t^s = i_t / \delta_t, \quad (41)$$

$$d_t = \alpha_t y_t - (1 + \varphi_t / \delta_t) i_t, \quad (42)$$

where I have made use of equation (19) and the budget relationships  $y_t/c_t = 1 + \delta_t x_t/\eta_t$ , and  $i_t/c_t = \delta_t x_t/\eta_t$ .

Notice that the factor distribution shock  $\alpha_t$  appears either directly or indirectly in equations (35) through (42). Efforts to explain movements in these variables using an otherwise similar model with  $\alpha_t = \bar{\alpha}$  for all  $t$  could therefore distort the importance of the other model shocks.

The equilibrium paths of  $p_{s,t}$  and  $d_t$  pin down the real equity return  $r_{s,t}$ . The equilibrium paths of the bond prices  $p_{b,t}$  and  $p_{c,t}$  are obtained by solving equations (22) and (23). The solutions, which pin down the real bond returns  $r_{b,t}$  and  $r_{c,t}$ , are contained in Appendix B.

### 3 Parameter values

Figure 2 plots the U.S. data versions of ten model variables. The sources and methods used to construct these variables, plus the long-term bond return, are described in Appendix D. Table 1 shows that six U.S. macroeconomic ratios are all close to their full-sample means in 1972.Q3. As an alternative to estimation, I calibrate parameter values so that the steady state or trend values of the model variables are exactly equal to the values observed in the data in 1972.Q3.<sup>27</sup> Table 2 summarizes the model parameter values.

Table 1. U.S. macroeconomic ratios, 1960.Q1 to 2022.Q4

Ratio	$c_t/y_t$	$i_t/y_t$	$k_t/y_t$	$r_t k_t/y_t$	$p_{s,t}/y_t$	$d_t/y_t$
1972.Q3 value	0.713	0.287	9.243	0.361	4.216	0.040
Mean	0.727	0.273	9.190	0.383	4.018	0.036
Std. Dev.	0.018	0.018	0.411	0.027	1.501	0.012

Table 2. Model parameter values

Parameter	Value	Description/Target
$\bar{\eta}$	1	Risk aversion coefficient = 1 in 1972.Q3
$\gamma$	1	Frisch labor supply elasticity = $1/\gamma = 1$ .
$\bar{\alpha}$	0.361	Capital income share = 0.361 in 1972.Q3.
$A$	0.999	$k_t/y_t = 9.243$ with $y_t = 1$ and $z_t = 0$ in 1972.Q3.
$\bar{\delta}$	0.068	$i_t/y_t = 0.287$ in 1972.Q3.
$\bar{\varphi}$	0.008	$d_t/y_t = 0.040$ in 1972.Q3.
$B$	1.341	$B(i_t/k_t)^{\delta t} [\exp(z_t) h_{2,t}/k_t]^{\varphi t} = \exp(\mu)$ in 1972.Q3.
$D$	10.482	$h_{1,t} + h_{2,t} = 0.3$ in 1972.Q3.
$\bar{s}$	-0.225	$p_{s,t}/y_t = 4.216$ in 1972.Q3.
$\beta$	0.9998	$r_{b,t} = 0.248\%$ in 1972.Q3.
$\bar{\delta}_c$	0.944	$r_{c,t} = 0.872\%$ in 1972.Q3.

The steady state value  $\bar{\eta} = 1$  implies  $\bar{\kappa} = 0$  such that the agent’s utility function exhibits no habit component in steady state. The value of  $\gamma$  is chosen to deliver an aggregate Frisch labor supply elasticity of  $1/\gamma = 1$ . This value is consistent with empirical evidence presented by Kneip, Merz, and Storjohann (2020) who estimate an aggregate Frisch elasticity that ranges between 0.85 and 1.06 using panel data on German men from 2000 to 2013. Given a time endowment normalized to one, the value of the parameter  $D$  achieves the steady state target  $h_{1,t} + h_{2,t} = 0.3$ , implying that the representative agent spends about one-third of available time engaged in market work or investor effort. The values of the parameters  $A$  and  $B$  achieve

<sup>27</sup>Many studies, such as Smets and Wouters (2007), Christiano, Motto, and Rostagno (2014), and Miao, Wang, and Xu (2015) employ a combination of calibration and estimation to pin down their model’s parameter values. While estimation is typically viewed as more rigorous than calibration, Meenagh, Minford, and Wickens (2021) show that Bayesian and maximum likelihood estimation methods can both deliver significantly biased estimates of the true model’s parameter values.

the steady state targets of  $k_t/y_t = 9.243$  and  $k_{t+1}/k_t = \exp(\mu)$  in 1972.Q3 when  $y_t = 1$  and  $z_t = 0$ , as implied by equations (6) and (11).

The model-implied values of  $p_{s,t}/y_t$  and  $r_{b,t}$  in 1972.Q3 depend on numerous model parameters, including  $\bar{s}$ ,  $\beta$ , and various shock variances which are determined by the data replication exercise (for details, see Appendices A and B). Given candidate shock sequences and their corresponding variances, the values of  $\bar{s}$  and  $\beta$  are determined iteratively until the model-implied values for  $p_{s,t}/y_t$  and  $r_{b,t}$  match the corresponding values in U.S. data and the shock sequences have converged. The resulting value  $\bar{s} = -0.225$  in 1972.Q3 implies that equity sentiment is “pessimistic” relative to fundamental value in steady state. As noted in the introduction, this feature allows the model to replicate the mean equity risk premium in the data without the need for high levels of risk aversion. In section 5.2, I examine the sensitivity of the model’s mean asset returns to alternative values of  $\bar{s}$ .<sup>28</sup>

I solve for the sequences of shock realizations that allow the calibrated model to exactly replicate the observed time paths of eleven U.S. macroeconomic variables and asset returns. These are the ten time series plotted in Figure 2 plus the real return on a long-term U.S. Treasury bond. Of these eleven time series, only nine are independent since  $y_t = c_t + i_t$  and  $r_{s,t} = (p_{s,t} + d_t)/p_{s,t-1} - 1$ . The model has nine shocks, so each shock series is uniquely identified. The nine model shocks are:  $s_t$  (equity sentiment),  $\eta_t$  (risk aversion),  $u_t$  (labor disutility),  $v_t$  (capital law multiplier),  $\delta_t$  (capital law exponent on investment),  $\varphi_t$  (capital law exponent on investor effort),  $\alpha_t$  (factor distribution),  $z_t$  (labor productivity), and  $\omega_t$  (bond coupon decay rate). Appendix C provides the details of the shock identification procedure.<sup>29</sup>

Table 3 shows the values of the shock parameters implied by the identification exercise. The persistence parameters are computed by running an ordinary least squares regression on each shock sequence with the constant term constrained to coincide with the steady state value in 1972.Q3. The shock innovations are then computed using the univariate law of motion for each shock. All nine shocks exhibit very strong persistence—a typical result in the business cycle literature.<sup>30</sup> The strong shock persistence allows model variables that are presumed stationary (e.g., hours worked per person, capital’s share of income, and the equity value-consumption ratio) to be able to replicate the sustained upward or downward trends observed in U.S. data.

---

<sup>28</sup>In a similar framework with only six fundamental shocks, Lansing (2019) sets  $\bar{s} = 0$ . That version of the model cannot replicate the U.S. equity risk premium or the risk free rate of return.

<sup>29</sup>For similar shock identification exercises, but in the context of different models, see Lansing and Markiewicz (2018), Gelain, Lansing, and Natvik (2018), Buckman, et al. (2020), and Lansing (2021).

<sup>30</sup>See, for example, Christiano, Motto, and Rostagno (2014, p. 44).

Table 3. Model-identified shock parameters

Shock	Values	
Equity sentiment, $s_t$	$\rho_s = 0.9432$	$\sigma_{\varepsilon,s} = 0.1039$
Risk aversion, $\eta_t$	$\rho_\eta = 0.8987$	$\sigma_{\varepsilon,\eta} = 0.1248$
Labor disutility, $u_t$	$\rho_u = 0.9480$	$\sigma_{\varepsilon,u} = 0.1305$
Capital law multiplier, $v_t$	$\rho_v = 0.9808$	$\sigma_{\varepsilon,v} = 0.0363$
Capital law exponent on investment, $\delta_t$	$\rho_\delta = 0.9825$	$\sigma_{\varepsilon,\delta} = 0.0840$
Capital law exponent on investor effort, $\varphi_t$	$\rho_\varphi = 0.9916$	$\sigma_{\varepsilon,\varphi} = 0.1390$
Factor distribution, $\alpha_t$	$\rho_\alpha = 0.9968$	$\sigma_{\varepsilon,\alpha} = 0.0138$
Labor productivity, $z_t$	$\mu = 0.0050$	$\sigma_{\varepsilon,z} = 0.0233$
Bond coupon decay rate, $\omega_t$	$\rho_\omega = 0.9836$	$\sigma_{\varepsilon,\omega} = 0.0064$

## 4 Model-identified shocks

Figure 3 plots the nine model-identified shock sequences. By construction, all shocks are equal to their steady state or trend values in 1972.Q3.<sup>31</sup> The equity sentiment shock fluctuates between  $-0.98$  and  $0.05$ , thereby allowing the model to replicate movements in the U.S. ratio  $p_{s,t}/y_t$ . As described in Appendix D,  $p_{s,t}/y_t$  is the nominal market capitalization of the S&P 500 stock price index divided by a model-consistent measure of nominal output. The sentiment shock reaches its two highest values in 2001.Q1 and 2001.Q4, near the peak of the NASDAQ technology stock boom. The two lowest values occur during the recession quarters of 1982.Q3 and 2009.Q2.

The risk aversion coefficient  $\eta_t$  fluctuates mildly between  $0.46$  and  $1.32$ , thereby allowing the model to replicate the smooth behavior of the U.S. risk free rate of return, as plotted in Figure 2.<sup>32</sup> The maximum value occurs in 2001.Q4 while the minimum value occurs in 1982.Q3. Movements in  $\eta_t$  exhibit a strong positive correlation with movements in  $s_t$ . As demonstrated below in Section 5.3, this correlation pattern allows the model to match the comovement of U.S. macroeconomic variables and asset prices over the business cycle.

The labor disutility shock  $u_t$  exhibits a net downward trend over time, allowing the model to match the net upward trend of total hours worked per person in the data, as shown earlier in Figure 2. The net upward trend in  $h_t$  occurs despite the net downward trend in labor's share of income that results from the net increase in the factor distribution shock  $\alpha_t$ . Movements in  $u_t$  are positively correlated with movements in  $s_t$  and  $\eta_t$ . This correlation pattern allows the model to match both the amplitude and comovement of macroeconomic variables and asset prices over the business cycle.

<sup>31</sup>The trend value of  $z_t$  is constructed as  $\bar{z}_t = \bar{z}_{t-1} + \mu$ , where  $\mu$  is the sample mean of  $\Delta z_t$  and  $\bar{z}_t = z_t = 0$  in 1972.Q3.

<sup>32</sup>As noted by Cochrane (2017, p. 947), a risk aversion coefficient of 25 under power utility would imply that a 1 percentage point rise in mean consumption growth results in a 25 percentage point rise in the risk-free rate.

The multiplier shock  $v_t$  in the capital law of motion (11) is positively correlated with the other two capital law of motion shocks  $\delta_t$  and  $\varphi_t$ .<sup>33</sup> Consequently,  $v_t$  is almost perfectly negatively correlated with the quantity  $1 - \delta_t - \varphi_t$ , representing the exponent on  $k_t$  in the capital law of motion. This correlation pattern allows the model to match the smooth time path of  $k_t$  in the data while simultaneously matching the more-volatile time paths of  $i_t$  and  $p_{s,t} = i_t/\delta_t$ . Fluctuations in the investor effort shock  $\varphi_t$  allow the model to match the time path of  $d_t$  in the data. The positive correlation between innovations to  $\delta_t$  and  $\varphi_t$  allows the model to replicate the comovement between  $p_{s,t}$  and  $d_t$  in the data.

The factor distribution shock  $\alpha_t$ , representing capital’s share of income, fluctuates around its steady state value until experiencing a sustained upward trend starting around 2005. As described in Appendix D,  $\alpha_t$  is measured as one minus the ratio of employee compensation to gross value added of the corporate business sector.<sup>34</sup> A study by Bergholt, Furlanetto, and Maffei-Faccioli (2022) finds that automation and rising markups of firms’ prices are the main drivers of the rise in the U.S. capital income share.

The labor productivity shock  $z_t$  evolves close to trend from around 1970 until the onset of Great Recession in 2008. The shock remains well below trend at the end of the data sample in 2022.Q4. The decline in  $z_t$  after the Great Recession partially offsets the concurrent rise in  $\alpha_t$  so as to replicate the path of U.S. output. But even before 2005, innovations to these two shocks are strongly negatively correlated. Figure 4 also plots an alternative sequence for  $z_t$  that is identified by an otherwise similar Cobb-Douglas production function with  $\alpha_t = \bar{\alpha}$  for all  $t$ . The alternative sequence for  $z_t$  is very different from the model-identified sequence from 2005 onward. The correlation coefficient between innovations to  $\alpha_t$  and innovations to the alternative sequence for  $z_t$  is positive at 0.22. Given that  $\alpha_t$  appears either directly or indirectly in equations (35) through (42), imposing  $\alpha_t = \bar{\alpha}$  would also yield different sequences for the other model-identified shocks. This example illustrates how details of the assumed model can influence the patterns of identified shocks.

Finally, the bond coupon decay rate shock  $\omega_t$  exhibits a net upward trend over time. This pattern allows the model to match the net increase in the real return on a long-term Treasury bond that derives mainly from the secular decline in U.S. inflation. The value of  $\omega_t$  drops sharply at the end of the data sample, coinciding with a surge in U.S. inflation that acts to

---

<sup>33</sup>Throughout the paper, I refer to  $v_t$ ,  $\delta_t$ , and  $\varphi_t$  as the “capital law of motion shocks” because these shocks only appear in equation (11). While the labor productivity shock  $z_t$  also appears in equation (11), it has only minor effects on  $k_{t+1}$  because the investor effort shock  $\varphi_t$  fluctuates at very low values that range between 0.003 and 0.058. Movements in total labor hours  $h_t$  are dominated by movements in  $h_{1,t}$ . The average value of the ratio  $h_{1,t}/h_t$  in U.S. data from 1960.Q1 to 2022.Q4 is 0.89.

<sup>34</sup>Fernald (2014) uses smoothed quarterly data on capital’s share of income to identify a quarterly time series for total factor productivity using a Cobb-Douglas production function. The correlation coefficient between  $\alpha_t$  and Fernald’s measure of capital’s share is 0.986 using updated data available from <https://www.johnfernal.net/TFP>.

reduce the real return on the U.S. long-term bond. Movements in  $\omega_t$  over time also allow the model to capture the shifting correlation pattern between returns on bonds versus equities, as documented by Campbell, Pflueger, and Viceira (2020).

Table 4 compares the standard deviation of the model-identified shock innovations before and after 1984. This date corresponds to the approximate start of what had previously been labeled as the “Great Moderation” (e.g., Stock and Watson 2002). Innovation volatility declines in the post-1984 sub-sample for the three capital law of motion shocks  $v_t$ ,  $\delta_t$ , and  $\varphi_t$ . But for the remaining six shocks, innovation volatility rises in the post-1984 sub-sample, particularly for the two production function shocks  $\alpha_t$  and  $z_t$ . Qualitatively similar results are obtained if the second sub-sample ends in 2019.Q4 to avoid the influence of the severe but brief Covid recession. Overall, the results in Table 4 do not support the notion that macroeconomic or financial volatility has declined in recent decades.

Table 4. Standard deviation of shock innovations

Innovation	1960.Q2 to 1983.Q4	1984.Q1 to 2022.Q4	Change
$\varepsilon_{s,t}$	0.1008	0.1060	+5.15%
$\varepsilon_{\eta,t}$	0.1244	0.1253	+0.71%
$\varepsilon_{u,t}$	0.1287	0.1320	+2.54%
$\varepsilon_{v,t}$	0.0371	0.0357	-3.71%
$\varepsilon_{\delta,t}$	0.0878	0.0808	-8.03%
$\varepsilon_{\varphi,t}$	0.1547	0.1286	-16.9%
$\varepsilon_{\alpha,t}$	0.0120	0.0148	+23.9%
$\varepsilon_{z,t}$	0.0177	0.0260	+47.4%
$\varepsilon_{\omega,t}$	0.0057	0.0069	+21.2%

Note: Last column is the percent change in volatility from pre- to post-1984 sample periods.

Table 5 shows the contemporaneous cross correlations among the nine shock innovations. There are strong positive correlations between  $\varepsilon_{s,t}$  (sentiment),  $\varepsilon_{\eta,t}$  (risk aversion), and  $\varepsilon_{u,t}$  (labor disutility). There are also strong positive correlations between  $\varepsilon_{v,t}$ ,  $\varepsilon_{\delta,t}$ , and  $\varepsilon_{\varphi,t}$  (capital law of motion). The first group of innovations is negatively correlated with the second group. There is a strong negative correlation between  $\varepsilon_{\alpha,t}$  (factor distribution) and  $\varepsilon_{z,t}$  (labor productivity), but these two innovations are mostly weakly correlated with the other innovations. While there are sizeable positive correlations between  $\varepsilon_{\omega,t}$  (bond coupon decay rate) and the first group of innovations noted above, the coupon decay shock only reacts to these innovations; it does not influence the evolution of the macroeconomic variables or other asset prices.

The correlation patterns in Table 5 motivate three categories of shocks for the counterfactual scenarios: (1) only sentiment and preference shocks:  $s_t$ ,  $\eta_t$ , and  $u_t$ , (2) only capital law of motion shocks:  $v_t$ ,  $\delta_t$ , and  $\varphi_t$ , and (3) only production function shocks:  $\alpha_t$  and  $z_t$ . These categories roughly correspond to the three main building blocks of the model, namely,

the household utility function, the law of motion for capital, and the production function for output.<sup>35</sup> The counterfactual scenarios will seek to isolate the main source of fluctuations as roughly coming from either household demand factors, financial factors that influence capital formation, or production/supply factors.

Table 5. Contemporaneous cross correlations of shock innovations

Innovation	$\varepsilon_{s,t}$	$\varepsilon_{\eta,t}$	$\varepsilon_{u,t}$	$\varepsilon_{v,t}$	$\varepsilon_{\delta,t}$	$\varepsilon_{\varphi,t}$	$\varepsilon_{\alpha,t}$	$\varepsilon_{z,t}$	$\varepsilon_{\omega,t}$
$\varepsilon_{s,t}$	1.00	<b>0.98</b>	<b>0.97</b>	-0.62	-0.38	-0.36	-0.19	0.31	0.68
$\varepsilon_{\eta,t}$		1.00	<b>0.97</b>	-0.51	-0.26	-0.29	-0.13	0.26	0.70
$\varepsilon_{u,t}$			1.00	-0.50	-0.28	-0.28	-0.18	0.31	0.73
$\varepsilon_{v,t}$				1.00	<b>0.89</b>	<b>0.66</b>	0.12	-0.13	-0.12
$\varepsilon_{\delta,t}$					1.00	<b>0.51</b>	-0.04	0.05	-0.03
$\varepsilon_{\varphi,t}$						1.00	0.46	-0.38	-0.10
$\varepsilon_{\alpha,t}$							1.00	<b>-0.89</b>	-0.20
$\varepsilon_{z,t}$								1.00	0.28
$\varepsilon_{\omega,t}$									1.00

Note: Correlation coefficients computed for the sample period from 1960.Q2 to 2022.Q4. Bold entries indicate strong correlations that motivate the three main shock categories for counterfactual scenarios.

Recall that the boundedly-rational agent in the model employs univariate forecast rules for each of the nine shocks. Under full information rational expectations, the agent would employ forecast rules that capture the complex correlation structure in Table 5. Appendix E examines the potential improvement in forecast accuracy from taking into account the shock correlation structure. Specifically, I compare the accuracy of the model’s univariate forecast rules to the accuracy of forecasts derived from a 1-lag VAR estimated on the nine model-identified shock sequences. Use of the ex post estimated VAR delivers only minor improvements in the accuracy of the shock forecasts. The univariate shock forecasts are almost perfectly correlated with the VAR shock forecasts, confirming that the univariate forecast rules are near rational.

## 5 Quantitative properties of the model

### 5.1 Actual versus perceived law of motion

Figure 4 provides insight into the near self-fulfilling nature of the agent’s perceived law of motion (28). The left panel plots the equilibrium quantity  $\log(q_t/q_t^f)$  versus the value of the sentiment shock  $s_t$ . For this exercise, all fundamental shocks are set to their steady state values. The agent’s perceived law of motion predicts that  $\log(q_t/q_t^f)$  should increase with  $s_t$  along the 45-degree line with slope = 1. The actual law of motion implies that  $\log(q_t/q_t^f)$  increases along

<sup>35</sup>While the equity sentiment shock  $s_t$  does not enter directly in the household utility function it strongly comoves with the two preference shocks  $\eta_t$  and  $u_t$ .

a line with slope  $\simeq 0.9$ . For any given value of  $s_t$ , the value of  $\log(q_t/q_t^f)$  predicted by the two lines are numerically very close. For example when  $s_t = \bar{s}$ , the perceived law of motion predicts  $\log(q_t/q_t^f) = -0.225$  whereas the actual law of motion predicts  $\log(q_t/q_t^f) = -0.207$ .

The close approximation of the PLM to the ALM occurs because the slope coefficient applied to the agent’s subjective forecast  $\tilde{E}_t q_{t+1}$  in the transformed first order condition (25) is always close to 1, as given by  $[1 - \delta_t (1 - \alpha_t) - \varphi_t] \beta$ . From 1960.Q1 to 2022.Q4, the slope coefficient fluctuates between 0.85 and 0.97 with a steady state value of 0.95. Consequently, the agent’s subjective forecast has a very strong influence on the actual value of  $q_t$ .

## 5.2 Effect of steady state sentiment

The value  $\bar{s} = -0.225$  allows the model to replicate the equity risk premium in U.S. data while maintaining a low level of risk aversion. Table 6 shows the sensitivity of the model’s mean asset returns to higher values of sentiment in each period. Specifically, I shift up the entire sequence of model-identified sentiment shocks by a constant amount so as to achieve the steady state value  $\bar{s}' > \bar{s}$  in 1972.Q3. The sequences of the eight fundamental shocks are unchanged from the baseline model.

Table 6. Effect of steady state sentiment on mean asset returns

Steady state sentiment	$r_{s,t}$	$r_{b,t}$	$r_{c,t}$	$r_{s,t} - r_{b,t}$	$r_{s,t} - r_{c,t}$	$r_{c,t} - r_{b,t}$
$\bar{s} = -0.225$ , Baseline model	2.04	0.37	0.98	1.67	1.06	0.61
$\bar{s}' = -0.1$	1.33	0.72	1.19	0.61	0.13	0.48
$\bar{s}' = 0$	0.83	1.00	1.38	-0.17	-0.55	0.38
$\bar{s}' = 0.1$	0.39	1.28	1.58	-0.89	-1.18	0.29
$\bar{s}' = 0.225$	-0.08	1.64	1.84	-1.72	-1.92	0.20

Notes: Each number is the mean quarterly real return (measured in percent) from 1960.Q2 to 2022.Q4 under a given steady state value of the equity sentiment shock in 1972.Q3. The top row shows the mean quarterly returns in U.S. data that are matched in the baseline model with the shock realizations  $s_t$ . Other rows use the shock realizations  $s'_t = s_t + (\bar{s}' - \bar{s})$ , such that  $s'_t = \bar{s}'$  in 1972.Q3.

As  $\bar{s}'$  increases, the equity return  $r_{s,t}$  declines. At the same time, both bond returns rise, with the risk free rate  $r_{b,t}$  increasing by more than the long-term bond return  $r_{c,t}$ . Increased optimism serves to shrink, and eventually eliminate, both the mean equity risk premium and the mean bond term premium. For example, when sentiment is neutral in steady state such that  $\bar{s}' = 0$ , the mean equity risk premium relative to  $r_{b,t}$  is  $-0.17\%$  per quarter. In contrast, the baseline model with  $\bar{s} = -0.225$  delivers a mean equity risk premium of  $1.67\%$  per quarter.

## 5.3 Impulse response functions

Figure 5 plots three sets of impulse response functions from the model. Each set of panels show how macroeconomic variables and asset prices respond to positive innovations of one

standard deviation in size coming from each of the three main shock categories noted earlier. For illustrative purposes in this exercise, I set the persistence parameters for all shocks to a value of 0.9 so that the impulse response functions for each shock category decay over the same number of periods.

The left panels of Figure 5 shows the effects of simultaneous positive innovations to sentiment  $s_t$  and risk aversion  $\eta_t$ . Recall from Table 4 that there is a strong positive correlation between innovations to  $s_t$ ,  $\eta_t$ , and  $u_t$ . Higher sentiment together with higher risk aversion delivers a correlated increase in all macroeconomic variables. Equity value increases but bond prices decline, implying an increase in bond yields. The combination of these two highly correlated shocks allows the model to capture the features observed during a typical economic boom or recovery. Adding a simultaneous positive innovation to the labor disutility shock  $u_t$  serves to dampen the correlated upward movements in the macroeconomic variables and equity value, but has little effect on bond prices. Taken together, the positive correlations among the innovations to  $s_t$ ,  $\eta_t$ , and  $u_t$  allow the model to replicate both the amplitude and comovement of fluctuations in U.S. macroeconomic variables and asset prices.

Recall that higher risk aversion in the model derives from a higher value for the time-varying coefficient  $\kappa_t$  that multiplies the external reference level of consumption. The model-identified value of  $\kappa_t$  implies that agents place more emphasis on interpersonal consumption comparisons during good times. The fact that model-identified risk aversion is higher during good times provides a fundamental justification for investors' higher expectations of future stock market returns during good times, as measured by surveys (Figure 1). As discussed in the introduction, several empirical studies find evidence of pro-cyclical risk aversion using data on option prices for the S&P 500 stock index.

The middle panels of Figure 5 show the effects of a positive innovation to the factor distribution shock  $\alpha_t$ , representing an increase in capital's share of income. An increase in  $\alpha_t$  delivers a response pattern that is very similar to that shown in the left panels of Figure 5, except that hours worked now undergoes a small decline. Recall from Table 4 that there is a strong negative correlation between innovations to the two production function shocks  $\alpha_t$  and  $z_t$ . Adding a simultaneous negative innovation to the labor productivity shock  $z_t$  serves to dampen the responses of most variables without changing the basic pattern.<sup>36</sup>

The right panels of Figure 5 show the effects of simultaneous positive innovations to the three capital law of motion shocks  $v_t$ ,  $\delta_t$  and  $\varphi_t$ , as motivated by the correlation patterns in Table 4. The innovations deliver an immediate increase in output, hours worked, and investment. But since the capital stock cannot respond immediately, the initial increase in output is not sufficient to allow both consumption and investment to increase on impact. Consump-

---

<sup>36</sup>Due to the logarithmic utility function in consumption (1), any innovation to  $z_t$  generates exactly offsetting income and substitution on hours worked, leaving the response pattern for  $h_t$  unchanged.

tion drops slightly on impact, but then increases as the capital stock rises in response to the higher value of the multiplier shock  $v_t$  and higher investment. Overall, the exercise leads to a correlated increase in the macroeconomic variables. Notice however that equity value, given by  $p_{s,t} = i_t/\delta_t$ , declines on impact (with bond prices) but then rises with investment. This happens because the higher value of the shock  $\delta_t$  dominates the initial increase in investment, but the subsequent rise in investment pushes up  $p_{s,t}$ .

The main takeaway from Figure 5 is that each of the three main shock categories can generate all or most of the features of a typical business cycle. I will elaborate further on this point below.

## 6 Counterfactual shock scenarios

In this section, I undertake business cycle accounting exercises that involve counterfactual shock scenarios. Each scenario adds one category of shock realizations while other shocks are set equal to steady state or trend values. Any shock innovation variance terms that appear as constants in the model's equilibrium solution remain in place, regardless of the scenario. This procedure ensures that the values of the endogenous variables in 1972.Q3 remain fixed across counterfactual scenarios.<sup>37</sup> The agent's forecasts of future shock values that determine the model solution are based on univariate forecast rules, so omitting any given sequence of shock realizations does not affect the model solution or the agent's forecasts for the remaining shocks. Each counterfactual simulation starts at the model steady state in 1972.Q3 and then uses the model solution to compute the counterfactual values of model variables before and after 1972.Q3. To compute the counterfactual values before 1972.Q3, I invert the capital law of motion (11) to solve for  $k_t$  as a function of  $k_{t+1}$ ,  $i_t$ ,  $h_{2,t}$ ,  $v_t$ ,  $\delta_t$ ,  $\varphi_t$  and  $z_t$ .

### 6.1 Business cycle importance of shocks

To gauge the importance of each shock category for business cycle fluctuations, I compute the correlation coefficient between a detrended model variable under a given shock scenario and the detrended U.S. variable. The detrended paths are constructed by taking logarithms and applying the Hodrick-Prescott filter with a smoothing parameter of 1600.<sup>38</sup> The counterfactual scenarios represent each of the three main shock categories in isolation, plus a separate scenario involving only the bond coupon decay shock. Table 7 summarizes the results for five

---

<sup>37</sup>For example, equation (31) shows that the value of  $\bar{q}$  in 1972.Q3 is influenced by numerous innovation variance terms.

<sup>38</sup>Similar results are obtained if a shock category's importance is ranked by the fit of a regression that projects the detrended U.S. variable onto a constant and the detrended model variable.

macroeconomic variables:  $y_t$ ,  $c_t$ ,  $i_t$ ,  $h_t$ ,  $k_t$ , and three asset prices:  $p_{s,t}$ ,  $p_{b,t}$ ,  $p_{c,t}$ . A boldface entry in the table indicates the largest correlation coefficient for each variable.

Table 7. Model versus data correlation coefficients: Detrended variables

Shock scenario	$y_t$	$c_t$	$i_t$	$h_t$	$k_t$	$p_{s,t}$	$p_{b,t}$	$p_{c,t}$
Baseline model = U.S. data	1.00	1.00	1.00	1.00	1.00	1.00	1.00	1.00
Only sentiment & preference shocks	<b>0.69</b>	0.47	<b>0.67</b>	<b>0.98</b>	0.09	0.71	<b>0.53</b>	-0.21
Only capital law of motion shocks	0.40	0.16	0.45	-0.17	<b>0.49</b>	<b>0.96</b>	0.17	0.15
Only production function shocks	0.52	<b>0.71</b>	0.22	-0.16	0.24	0.22	0.10	-0.15
Only bond coupon decay shock	0.14	0.06	0.18	0.10	0.07	0.04	0.04	<b>0.84</b>

Notes: Each number is the correlation coefficient between the detrended path of the model variable under a given shock scenario and the detrended path of the U.S. data variable. Each scenario adds one category of shock realizations while other shocks are set equal to steady state or trend values. Boldface indicates the largest correlation coefficient for each variable.

In Table 7, each of the three main shock categories is the most important driver of at least one macroeconomic variable or asset price. For example, the sentiment and preference shocks are the most important drivers of business cycle movements in output, investment, hours worked, and the price of the short-term bond (which determines the risk free rate of return). Recall that this category of shocks includes the time-varying risk aversion coefficient and the labor disutility shock. The capital law of motion shocks are the most important drivers of business cycle movements in the capital stock and equity value. The production function shocks are the most important drivers of business cycle movements in consumption. But none of the three main shock categories can account for movements in the price of the long-term bond. Rather, this asset price is driven mainly by the highly-specific coupon decay shock. This last result tell us that movements in the price of a long-term U.S. Treasury bond cannot be readily explained by shocks that account for movements in the S&P 500 stock index or movements in the price of a short-term Treasury bond.

Table 7 further shows that each of the three main shock categories can deliver sizeable correlation coefficients for more than one variable. For detrended output, the correlation coefficients across the three main shock scenarios range from 0.40 to 0.69. For detrended equity value, the correlation coefficients range from 0.22 to 0.96, but the ordering across scenarios is now different.

Figure 6 compares the detrended paths of model output and model equity value (red lines) to the corresponding U.S. data (black lines) for each of the three main shock categories. The results confirm that business cycle movements in U.S. output and equity value can be plausibly driven by multiple types of shocks.

Chari, Kehoe, and McGrattan (2007) conclude that wedges involving labor productivity and labor supply are the main drivers of business cycles. For comparison with the results pre-

sented here, a labor productivity wedge would fall into the production function category while a labor supply wedge would fall into the sentiment and preference category. Table 7 shows that both of these shock categories can deliver sizeable correlation coefficients for detrended output and consumption. But production function shocks deliver only weak correlation coefficients for detrended asset prices.

Justiniano, Primiceri, and Tambalotti (2010) conclude that investment shocks are the main drivers of business cycle movements in output, hours, and investment. Table 7 shows that the capital law of motion shocks can indeed deliver sizeable correlation coefficients for detrended output, investment, and equity value, but not for detrended hours worked or detrended bond prices. Unlike the setup in Justiniano, Primiceri, and Tambalotti (2010), shocks to the capital law of motion in the model developed here are tasked with explaining movements in equity value and equity dividends, leaving the task of explaining hours worked and bond prices to other shocks.

## 6.2 Importance of shocks without detrending

To gauge the importance of each shock category for lower frequency movements, I first compute the squared percentage gaps between the counterfactual model paths and the U.S. data paths for each variable, without any detrending. A smaller gap measure implies that a given shock scenario does a better job of explaining total movements in a given U.S. variable. Following Brinca, et al. (2016), and Brinca, Costa-Filho, and Loria (2024), I then normalize the cumulative squared gaps across shock scenarios to construct an index that measures the fraction of total movements in each variable that can be explained by each shock scenario. For example, I compute the following gap accounting statistic for output  $y_t$

$$\theta_y^i = \frac{1/\sum_t (y_t^i/y_t - 1)^2}{\sum_j [1/\sum_t (y_t^j/y_t - 1)^2]}, \quad (43)$$

where  $\sum_t (y_t^i/y_t - 1)^2$  is the cumulative squared percentage gap that results from counterfactual shock scenario  $i$  and  $j = 3$  is the number of different shock scenarios. When all three shock categories are present, the gap is zero each period and the model can explain 100% of the total movements in each U.S. variable considered.<sup>39</sup>

Table 8 presents the gap accounting statistics for each variable. Figure 7 displays the counterfactual shock scenarios and the associated gaps for output  $y_t$  and equity value  $p_{s,t}$ . The scenario with only sentiment and preference shocks provides the best visual fit of fluctuations in U.S. output while the scenario with only capital law of motion shocks provides the best

---

<sup>39</sup>For this exercise, I do not compute a gap accounting statistic for the long-term bond price  $p_{c,t}$  because the highly-specific bond coupon decay shock  $\omega_t$  is not part of the three main shock categories that form the denominator of equation (43).

visual fit of fluctuations in U.S. equity value. These visual rankings are confirmed by the ranking of the gap accounting statistics in Table 8.

Table 8. Gap accounting statistics without detrending

Shock scenario	$y_t$	$c_t$	$i_t$	$h_t$	$k_t$	$p_{s,t}$	$p_{b,t}$
Baseline model = U.S. data	1.00	1.00	1.00	1.00	1.00	1.00	1.00
Only sentiment & preference shocks	<b>0.41</b>	0.35	<b>0.53</b>	<b>0.90</b>	0.40	0.12	0.11
Only capital law of motion shocks	0.29	0.28	0.35	0.06	<b>0.48</b>	<b>0.81</b>	0.14
Only production function shocks	0.30	<b>0.37</b>	0.12	0.04	0.12	0.07	<b>0.75</b>

Notes: Each number represents the fraction of total movements in a given U.S. variable that can be explained by each shock scenario, computed along the lines of equation (43). Boldface indicates the largest fraction for each variable.

From Table 8, we see that each of the three main shock categories can account for a sizeable fraction of total movements in the variables  $y_t$ ,  $c_t$ ,  $i_t$ , and  $k_t$ , implying that no single shock category is clearly dominant. In contrast, total movements in the variables  $h_t$ ,  $p_{s,t}$  and  $p_{b,t}$  are driven mainly by a single dominant shock category, but the dominant shock category is different for each variable. Specifically, the three largest gap accounting statistics in Table 8 are 0.90 for  $h_t$  with only sentiment and preference shocks, 0.81 for  $p_{s,t}$  with only capital law of motion shocks, and 0.75 for  $p_{b,t}$  with only production function shocks.

If we compare the correlation coefficients in Table 7 to the gap accounting statistics in Table 8, we see that the shock category which is the most important driver of business cycle movements in a given variable is usually, but not always, the most important driver of total movements in the same variable. The single exception is the short-term bond price  $p_{b,t}$ . In this case, the sentiment and preference shocks are the most important drivers of business cycle movements whereas the production function shocks are the most important drivers of total movements. Taken as a whole, the results in Tables 7 and 8 tell us that each of the three main shock categories is important for explaining aspects of U.S. data since 1960.

The scenario with only production function shocks delivers the lowest gap accounting statistic for equity value  $p_{s,t}$  at 0.07. Recall that this category of shocks includes  $\alpha_t$  which governs capital's share of income. Using concentrated capital ownership models (i.e., capital owners versus workers), studies by Lansing (2015), Greenwald, Lettau, and Ludvigson (2024), and Gaudio, Petrella, and Santoro (2023) all identify a large role for shocks to capital's share of income in explaining U.S. equity returns. The equity return in the concentrated capital ownership model is highly sensitive to the presence of factor distribution shocks because these shocks impact the volatility of equity dividends which, in turn, strongly influences the volatility of capital owners' consumption growth. But in the representative agent framework employed here, the same sequence of factor distribution shocks has much less impact on the volatility of the representative agent's consumption growth, thereby muting the resulting impact on equity

value and equity returns.<sup>40</sup> This example demonstrates that conclusions regarding the relative importance of any given shock for macroeconomic or financial variables can be model-specific.

### 6.3 Great Recession versus Covid recession

Previous business cycle accounting studies have shown that the main drivers of recessions can differ across episodes or countries. Brinca, et al. (2016) find that a labor wedge is the most important driver of the Great Recession in the U.S. but an efficiency wedge is the most important driver of the Great Recession in most other countries. Brinca, Costa-Filho, and Loria (2024) find that an efficiency wedge is the most important driver of the U.S. recessions in 1973 and 1990 which were characterized by spikes in oil prices.

As a final exercise, I assess how each shock scenario performs in explaining the Great Recession (2007.Q4 to 2009.Q2) versus the Covid recession (2019.Q4 to 2020.Q2). Starting from 2007.Q4, I add one category of shock realizations while other shocks are set equal to steady state or trend values. Figure 8 displays the counterfactual shock scenarios and the associated gaps for two key variables: output  $y_t$  and equity value  $p_{s,t}$ .

According to the model, the declines in  $y_t$  and  $p_{s,t}$  during the Great Recession are driven mainly by the capital law of motion shocks (red line) together with the sentiment and preference shocks (blue line). The importance of these two shock categories is consistent with the idea that both financial and demand factors played a significant role during the Great Recession, in line with the findings of Mian and Sufi (2010) and Gertler and Gilchrist (2018). The production function shocks do not contribute much to the declines in either  $y_t$  or  $p_{s,t}$  during the Great Recession, confirming the findings of Brinca, et al. (2016) with regard to the U.S. efficiency wedge.

The decline in  $y_t$  during the Covid recession is driven mainly by the sentiment and preference shocks (blue line) together with production function shocks (green line). The importance of these two shock categories is consistent with idea that both demand and supply factors played a significant role in the Covid recession, in line with the findings of Ferroni, Fisher, and Melosi (2024), Smets and Wouters (2024), and Bai, et al. (2024). The decline in  $p_{s,t}$  during the Covid recession is driven mainly by capital law of motion shocks (red line) together with production function shocks (green line). Overall, the results tell us that U.S. recessions can be driven by different types of shocks.

---

<sup>40</sup>This point is demonstrated numerically by Lansing (2015, p. 83) and Gaudio, Petrella, and Santoro (2023, p. 33).

## 7 Conclusion

I have used a standard real business cycle model to solve for the sequences of nine stochastic shocks (or wedges) that allow the model to exactly replicate the quarterly time paths of U.S. macroeconomic variables and asset returns since 1960. The model-identified sentiment shock is negative in steady state, allowing the model to match the U.S. equity risk premium with a low level of risk aversion. The model-identified risk aversion coefficient is higher in good times, when agents place more emphasis on interpersonal consumption comparisons. This pattern provides a justification for investors' higher expectations of future stock market returns during good times, as measured by surveys. It is also consistent with several empirical studies that estimate measures of time-varying risk aversion using option prices for the S&P 500 stock index.

The cross-correlation patterns among the identified shock innovations motivate three main shock categories as candidates for the most important driver of U.S. business cycles and asset returns: (1) sentiment and preference shocks, (2) capital law of motion shocks, and (3) production function shocks. These categories roughly correspond to the three main building blocks of the model: the household utility function, the law of motion for capital, and the production function for output.

Using impulse response functions, I show that each of the three main shock categories can generate all or most of the features of a typical business cycle. Counterfactual scenarios show that each of the three main shock categories is the most important driver of business cycle movements and total movements in at least one macroeconomic variable or asset price. For most variables, no single shock category is clearly dominant in explaining the observed movements in U.S. data. While some variables are driven by a single dominant shock category, the dominant category is different for each of those variables. Movements in the price of a long-term U.S. Treasury bond cannot be readily explained by shocks that account for movements in the S&P 500 stock index or movements in the price of a short-term Treasury bond. An analysis of the Great Recession versus the Covid recession shows that the shock categories which account for the declines in U.S. output and equity value differ across the two recession episodes.

The model incorporates a shock to capital's share of income which replicates fluctuations of this object in U.S. data. Models that do not allow for such shocks are likely to provide a distorted view of the importance of other model shocks. More generally, conclusions about the most important shock can be strongly influenced by the type of model, or the type of data, used in the exercise. Rather than continuing to search for the elusive "most important shock," it is perhaps time to conclude that the object of the search does not exist.

## References.

- Abel, A.B. (2002) An exploration of the effects of pessimism and doubt on asset returns, *Journal of Economic Dynamics and Control* 26, 1075-1092.
- Adam, K., A. Marcet, and J. Beutel (2017) Stock price booms and expected capital gains, *American Economic Review* 107, 2352-2408.
- Adam, K. and S. Merkel (2019) Stock price cycles and business cycles, European Central Bank Working Paper 2316.
- Adam, K., D. Matveev, and Stefan Nagel (2021) Do survey expectations of stock returns reflect risk adjustments? *Journal of Monetary Economics* 117, 723-740.
- Ambler, S. and A. Paquet (1994) Stochastic depreciation and the business cycle, *International Economic Review* 35, 101-116.
- Amromin, G., and S.A. Sharpe (2014) From the horse's mouth: Economic conditions and investor expectations of risk and return, *Management Science* 60, 845-866.
- Andrle, M. (2014) Estimating structural shocks with DSGE models, International Monetary Fund, Working Paper.
- Andrle, M., J. Brůha, and S. Solmaz (2017) On the sources of business cycles: Implications for DSGE models, European Central Bank Working Paper 2058.
- Angeletos, G.-M., F. Collard, and H. Dellas (2018) Quantifying confidence, *Econometrica* 86, 1689-1726.
- Angeletos, G.-M., F. Collard, and H. Dellas (2020) Business-cycle anatomy, *American Economic Review* 110, 3030-3070.
- Ascari, G. and S. Mavroeidis (2022) The unbearable lightness of equilibria in a low interest rate environment, *Journal of Monetary Economics* 127, 1-17.
- Bai, X., J. Fernández-Villaverde, Y. Li, and F. Zanetti (2024) The causal effects of global supply chain disruptions on macroeconomic outcomes: Evidence and theory, NBER Working Paper 32098.
- Baker, M. and J. Wurgler (2007) Investor sentiment in the stock market, *Journal of Economic Perspectives* 21(2), 129-152.
- Barone-Adesi, G., L. Mancini, and H. Shefrin (2107) Estimating sentiment, risk aversion, and time preference from behavioral pricing kernel theory, Swiss Finance Institute Research Paper No. 12-21. Available online at: <http://dx.doi.org/10.2139/ssrn.2060983>
- Barro, R.J. 2009 Rare disasters, asset prices, and welfare costs, *American Economic Review* 99, 243-264.
- Beaubrun-Diant, K.E. and F. Tripier (2005) Asset returns and business cycles in models with investment adjustment costs, *Economics Letters* 86, 141-146.
- Bergholt, D., F. Furlanetto, and N. Maffei-Faccioli (2022) The decline of the labor share: New empirical evidence, *American Economic Journal: Macroeconomics* 14(3), 163-198.
- Bernanke, B.S., M. Gertler, and S. Gilchrist (1999), The financial accelerator in a quantitative business cycle framework. In J. Taylor and M. Woodford (eds.), *Handbook of Macroeconomics*, pp. 1341-1393. Amsterdam: North-Holland.
- Bianchi, F., S.C. Ludvigson, and S. Ma (2022) Belief distortions and macroeconomic fluctuations, *American Economic Review* 112, 2269-2315.
- Bidder, R.M. and I. Dew-Becker (2016) Long-run risk is the worst-case scenario, *American Economic Review* 106, 2494-2527.
- Bhandari, A., J. Borovička, and P. Ho (2024) Survey data and subjective beliefs in business cycle models, *Review of Economic Studies*, forthcoming.

- Bliss, R. and N. Panigirtzoglou (2004) Option implied risk aversion estimates, *Journal of Finance* 59, 407-446.
- Brinca, P., V.V. Chari, P.J. Kehoe, and E. McGrattan (2016), Accounting for business cycles. In: J.B. Taylor and H. Uhlig (eds.) *Handbook of Macroeconomics, Volume 2A*, pp. 1013-1063. Amsterdam: North-Holland.
- Brinca, P., J. Costa-Filho, and F. Loria (2024) Business cycle accounting: What have we learned so far? *Journal of Economic Surveys*, forthcoming.
- Buckman, S.R., R. Glick, K.J. Lansing, N. Petrosky-Nadeau, and L.M. Seitelman (2020) Replicating and projecting the path of COVID-19 with a model-implied reproduction number, *Infectious Disease Modelling* 5, 635-651.
- Campbell, J.Y., C. Pflueger, and L.M. Viceira (2020) Macroeconomic drivers of bond and equity risks, *Journal of Political Economy* 128, 3148-3185.
- Campello, M. and J. Graham (2013) Do stock prices influence corporate decisions? Evidence from the technology bubble, *Journal of Financial Economics* 107, 89-110.
- Cecchetti, S.G., P.-S. Lam, and N.C. Mark (2000) Asset pricing with distorted beliefs: Are equity returns too good to be true? *American Economic Review* 90, 787-805.
- Chari, V.V., P.J. Kehoe, and E.R. McGrattan (2007) Business cycle accounting, *Econometrica* 75, 781-836.
- Chirinko, R.S. and H. Schaller (2001) Business fixed investment and ‘bubbles’: The Japanese case, *American Economic Review* 91, 663-680.
- Christiano, L.J., R. Motto, and M. Rostagno (2014) Risk shocks, *American Economic Review* 104, 27-65.
- Cochrane, J.H. (2017) Macro-Finance, *Review of Finance* 21, 945-985.
- Cogley, T. and T.J. Sargent (2008) The market price of risk and the equity premium: A legacy of the Great Depression? *Journal of Monetary Economics* 55, 454-476.
- Cúrdia, V. and R. Reis (2011) Correlated disturbances and the U.S. business cycle, NBER Working Paper 15774.
- Danthine, J.-P. and J.B. Donaldson (2002) Labour relations and asset prices, *Review of Economic Studies* 69, 41-64.
- Falter, A. and D. Wesselbaum (2018) Correlated shocks in estimated DSGE models, *Economics Bulletin* 38, 2026-2036.
- Fernald, J.G. (2014) A quarterly, utilization-adjusted series on total factor productivity, FRBSF Working Paper 2012-19.
- Ferroni, F., J.D.M. Fisher, and L. Melosi (2024) Unusual shocks in our usual models, *Journal of Monetary Economics*, forthcoming.
- Frydman, R. and J.R. Stillwagon (2018) Fundamental factors and extrapolation in stock-market expectations: The central role of structural change, *Journal of Economic Behavior and Organization* 148, 189-198.
- Furlanetto, F. and M. Seneca (2014), New perspectives on depreciation shocks as a source of business cycle fluctuations, *Macroeconomic Dynamics* 18, 1209-1233.
- Gaudio, F.S., I. Petrella, and E. Santoro (2023) Asset market participation, redistribution, and asset pricing, CEPR Discussion Paper 17984.
- Gelain, P., K.J. Lansing, and G.J. Natvik (2018) Explaining the boom-bust cycle in the U.S. housing market: A reverse-engineering approach, *Journal of Money Credit and Banking* 50, 1751-1782.
- Gertler, M. and S. Gilchrist (2018) What happened: Financial factors in the Great Recession, *Journal of Economic Perspectives* 32(3), 3-30.

- Giglio, S., M. Maggiori, J. Stroebel, and S. Utkus (2021). Five facts about beliefs and portfolios, *American Economic Review*, 111, 1481–1522.
- Gilchrist, S., C.P. Himmelberg, and G. Huberman (2005) Do stock price bubbles influence corporate investment? *Journal of Monetary Economics* 52, 805–827.
- Gourio, F. (2012) Disaster risk and business cycles, *American Economic Review* 102, 2734–2766.
- Goyal, V.K. and T. Yamada (2004) Asset price shocks, financial constraints, and investment: Evidence from Japan, *Journal of Business* 77, 175–200.
- Greenwald, D.L., M. Lettau and S.C. Ludvigson (2024) How the wealth was won: Factor shares as market fundamentals, *Journal of Political Economy*, forthcoming.
- Greenwood, J., Z. Hercowitz, and G.W. Huffman (1988) Investment, capacity utilization, and the real business cycle, *American Economic Review* 78, 402–417.
- Greenwood, R. and A. Shleifer (2014) Expectations of returns and expected returns, *Review of Financial Studies* 27, 714–746.
- Guvenen, F. (2009) A parsimonious macroeconomic model for asset pricing, *Econometrica* 77, 1711–1750.
- Hall, R.E. (1997), Macroeconomic fluctuations and the allocation of time, *Journal of Labor Economics* 15(1), S223–S250.
- Huang, D., F. Jiang, J. Tu, and G. Zhou (2014) Investor sentiment aligned: A powerful predictor of stock returns, *Review of Financial Studies* 28, 791–837.
- Iacoviello, M. (2005) House prices, borrowing constraints, and monetary policy in the business cycle, *American Economic Review*, 95 739–764.
- Jermann, U.J. (1998) Asset pricing in production economies, *Journal of Monetary Economics* 41, 257–275.
- Justiniano, A., G.E. Primiceri, and A. Tambalotti (2010), Investment shocks and business cycles, *Journal of Monetary Economics* 57, 132–145.
- Kaplan, G. and S. Schulhofer-Wohl (2018) The changing (dis-)utility of work, *Journal of Economic Perspectives* 32(3), 239–258.
- Keynes, J. M. (1936), *General Theory of Employment, Interest and Money*, London: Macmillan.
- Kocherlakota, N. (2010) Modern macroeconomic models as tools for economic policy, Federal Reserve Bank of Minneapolis, *The Region*, pp. 5–21.
- Kosolapova, M., M. Hanke and A. Weissensteiner (2023) Estimating time-varying risk aversion from option prices and realized returns, *Quantitative Finance* 23, 1–17..
- Kneip, A., M. Merz, and L. Storjohann (2020) Aggregation and labor supply elasticities, *Journal of the European Economic Association* 18(5), 2315–2358.
- Lansing, K.J. (2006) Lock-in of extrapolative expectations in an asset pricing model, *Macroeconomic Dynamics* 10, 317–348.
- Lansing, K.J. (2010) Rational and near-rational bubbles without drift, *Economic Journal* 120, 1149–1174.
- Lansing, K.J. (2012) Speculative growth, overreaction, and the welfare cost of technology-driven bubbles, *Journal of Economic Behavior and Organization* 83, 461–483.
- Lansing, K.J. (2015) Asset pricing with concentrated ownership of capital and distribution shocks, *American Economic Journal-Macroeconomics* 7, 67–103.
- Lansing, K.J. (2016) On variance bounds for asset price changes, *Journal of Financial Markets* 28, 132–148

- Lansing, K.J. (2019) Real business cycles, animal spirits, and stock market valuation, *International Journal of Economic Theory* 15, 77-94.
- Lansing, K.J. (2021) Endogenous forecast switching near the zero lower bound, *Journal of Monetary Economics* 117, 153-169.
- Lansing, K.J. and S.F. LeRoy (2014) Risk aversion, investor information, and stock market volatility, *European Economic Review* 70, 88-107.
- Lansing, K.J. and A. Markiewicz (2018) Top incomes, rising inequality, and welfare, *Economic Journal* 128, 262-297.
- Lansing, K.J., S.F. LeRoy, and J. Ma (2022) Examining the sources of excess return predictability: Stochastic volatility or market inefficiency? *Journal of Economic Behavior and Organization* 197, 50-72.
- LeRoy, S.F. and R.D. Porter (1981) The present-value relation: Tests based on implied variance bounds, *Econometrica* 49, 555-577.
- Liu, Z., D.F. Waggoner and T. Zha (2011) Sources of macroeconomic fluctuations: A regime-switching DSGE approach, *Quantitative Economics* 2, 251-301.
- Macnamara, P. (2016) Understanding entry and exit: A business cycle accounting approach. *B.E. Journal of Macroeconomics* 16(1), 47-91.
- Maurer, J. and A. Meier (2008) Smooth it like the ‘Joneses’? Estimating peer-group effects in intertemporal consumption choice, *Economic Journal* 118, 454-476.
- Meenagh, D., P. Minford and M.R. Wickens (2021) Estimating macro models and the potentially misleading nature of Bayesian estimation, CEPR Discussion Paper 15684.
- Mian, A. and A. Sufi (2010) The Great Recession: Lessons from microeconomic data, *American Economic Review: Papers and Proceedings* 100, 51-56.
- Miao, J., P. Wang, and Z. Xu. (2015) A Bayesian DSGE model of stock market bubbles and business cycles, *Quantitative Economics* 6, 599-635.
- Morley, J.C., C.R. Nelson, and E. Zivot (2003) Why are the Beveridge-Nelson and unobserved-components decompositions of GDP so different? *Review of Economics and Statistics* 85, 235-243.
- Nagel, S. and Z. Xu (2022a) Asset pricing with fading memory, *Review of Financial Studies* 35, 2190-2245.
- Nagel, S. and Z. Xu (2022b) Dynamics of subjective risk premia, NBER Working Paper 29803.
- Otrok, C., B. Ravikumar, and C.H. Whiteman (2002) Habit formation: A resolution of the equity premium puzzle? *Journal of Monetary Economics* 49, 1261-1288.
- Pigou, A.C. (1927) *Industrial Fluctuations*, London: Macmillan.
- Rietz, T.A. (1988) The equity risk premium: A solution, *Journal of Monetary Economics* 22, 117-131.
- Ríos-Rull, J.V. and R. Santaeulàlia-Llopis (2010) Redistribution shocks and productivity shocks, *Journal of Monetary Economics* 57, 931-948.
- Schmeling, M. (2009) Investor sentiment and stock returns: Some international evidence, *Journal of Empirical Finance* 16, 394-408.
- Shiller, R.J. (1981), Do stock prices move too much to be justified by subsequent changes in dividends? *American Economic Review* 71, 421-436.
- Smets, F. and R. Wouters (2007) Shocks and frictions in U.S. business cycles: A Bayesian DSGE approach, *American Economic Review* 97, 586-606.
- Smets, F. and R. Wouters (2024) “Fiscal Backing, Inflation, and U.S. Business Cycles,” Working Paper.

Stock, J.H. and M.W. Watson (2002) Has the business cycle changed and why? In: M. Gertler and K. Rogoff, (eds.), *NBER Macroeconomics Annual 2002*, pp. 159-218. Cambridge, MA: MIT Press.

Šustek, R. (2011) Monetary business cycle accounting, *Review of Economic Dynamics* 14, 592-612.

Velásquez-Giraldo, M. (2023) Life-Cycle Portfolio Choices and Heterogeneous Stock Market Expectations,” John Hopkins University, Working Paper.

Vissing-Jørgensen, A. (2004) Perspectives on behavioral finance: Does irrationality disappear with wealth? Evidence from expectations and actions. In: M. Gertler and K. Rogoff, (eds.), *NBER Macroeconomics Annual 2003*, pp. 139-194. Cambridge, MA: MIT Press.

Welch, I. and A. Goyal (2008) A comprehensive look at the empirical performance of equity premium prediction, *Review of Financial Studies* 21, 1455-1508.

Young, A.T. (2004) Labor’s share fluctuations, biased technical change, and the business cycle, *Review of Economic Dynamics* 7, 916-931.

Yu, J., 2013. A sentiment-based explanation for the forward premium puzzle, *Journal of Monetary Economics* 60, 474-491.

Zhu, X. (1995) Endogenous capital utilization, investor’s effort, and optimal fiscal policy, *Journal of Monetary Economics* 36, 655-677.

# Appendix

## A Fundamental equity value

This appendix provides details of the fundamental solution for  $q_t^f$  shown in equation (26). First imposing model-consistent expectations and then log-linearizing the right-side of the fundamentals-only version of the transformed first order condition (25) yields

$$q_t^f = b_0 \left[ \frac{\eta_t}{\bar{\eta}} \right]^{b_1} \left[ \frac{\alpha_t}{\bar{\alpha}} \right]^{b_2} \left[ \frac{\delta_t}{\bar{\delta}} \right]^{b_3} \left[ \frac{\varphi_t}{\bar{\varphi}} \right]^{b_4} E_t^m \left[ \frac{q_{t+1}^f}{\bar{q}^f} \right]^{b_5}, \quad (\text{A.1})$$

where  $b_i$  for  $i = 0$  to  $5$  are Taylor-series coefficients and  $\bar{q}^f \equiv \exp[E^m \log(q_t^f)]$ . The expressions for the Taylor-series coefficients are

$$b_0 = \bar{\alpha} \bar{\eta} + [1 - \bar{\delta}(1 - \bar{\alpha}) - \bar{\varphi}] \beta \bar{q}^f, \quad (\text{A.2})$$

$$b_1 = \frac{\bar{\alpha} \bar{\eta}}{\bar{\alpha} \bar{\eta} + [1 - \bar{\delta}(1 - \bar{\alpha}) - \bar{\varphi}] \beta \bar{q}^f}, \quad (\text{A.3})$$

$$b_2 = \frac{\bar{\alpha} (\bar{\eta} + \bar{\delta} \beta \bar{q}^f)}{\bar{\alpha} \bar{\eta} + [1 - \bar{\delta}(1 - \bar{\alpha}) - \bar{\varphi}] \beta \bar{q}^f}, \quad (\text{A.4})$$

$$b_3 = \frac{-\bar{\delta}(1 - \bar{\alpha}) \beta \bar{q}^f}{\bar{\alpha} \bar{\eta} + [1 - \bar{\delta}(1 - \bar{\alpha}) - \bar{\varphi}] \beta \bar{q}^f}, \quad (\text{A.5})$$

$$b_4 = \frac{-\bar{\varphi} \beta \bar{q}^f}{\bar{\alpha} \bar{\eta} + [1 - \bar{\delta}(1 - \bar{\alpha}) - \bar{\varphi}] \beta \bar{q}^f}, \quad (\text{A.6})$$

$$b_5 = \frac{[1 - \bar{\delta}(1 - \bar{\alpha}) - \bar{\varphi}] \beta \bar{q}^f}{\bar{\alpha} \bar{\eta} + [1 - \bar{\delta}(1 - \bar{\alpha}) - \bar{\varphi}] \beta \bar{q}^f}, \quad (\text{A.7})$$

A conjecture for the fundamental solution takes the form of equation (26). The conjectured solution is iterated ahead one period and then substituted into the right-side of equation (A.1) together with the laws of motion for  $\eta_{t+1}$ ,  $\alpha_{t+1}$ ,  $\delta_{t+1}$  and  $\varphi_{t+1}$  from equations (4), (8), (13) and (14), respectively. After evaluating the model-consistent expectation and then collecting terms, we have

$$q_t^f = \underbrace{b_0 \exp \left[ (\gamma_\eta b_5)^2 \sigma_{\varepsilon, \eta}^2 / 2 + (\gamma_\alpha b_5)^2 \sigma_{\varepsilon, \alpha}^2 / 2 + (\gamma_\delta b_5)^2 \sigma_{\varepsilon, \delta}^2 / 2 + (\gamma_\varphi b_5)^2 \sigma_{\varepsilon, \varphi}^2 / 2 \right]}_{=\bar{q}^f} \times \left[ \frac{\eta_t}{\bar{\eta}} \right]^{\underbrace{b_1 + \rho_\eta \gamma_\eta b_5}_{=\gamma_\eta}} \times \left[ \frac{\alpha_t}{\bar{\alpha}} \right]^{\underbrace{b_2 + \rho_\alpha \gamma_\alpha b_5}_{=\gamma_\alpha}} \times \left[ \frac{\delta_t}{\bar{\delta}} \right]^{\underbrace{b_3 + \rho_\delta \gamma_\delta b_5}_{=\gamma_\delta}} \times \left[ \frac{\varphi_t}{\bar{\varphi}} \right]^{\underbrace{b_4 + \rho_\varphi \gamma_\varphi b_5}_{=\gamma_\varphi}} \quad (\text{A.8})$$

which yields five equations in the five solution coefficients  $\bar{q}^f$ ,  $\gamma_\eta$ ,  $\gamma_\alpha$ ,  $\gamma_\delta$ , and  $\gamma_\varphi$ . For the baseline calibration, the resulting solution coefficients are  $\bar{q}^f = 7.342$ ,  $\gamma_\eta = 0.339$ ,  $\gamma_\alpha = 1.413$ ,  $\gamma_\delta = -0.660$ , and  $\gamma_\varphi = -0.142$ .

## B Equilibrium bond prices

This appendix outlines the solutions for the equilibrium bond prices  $p_{b,t}$  and  $p_{c,t}$  using equations (22) and (23). The equilibrium stochastic discount factor can be written as follows

$$\begin{aligned} M_{t+1} &= \beta \frac{\eta_{t+1}}{\eta_t} \times \frac{c_t/y_t}{c_{t+1}/y_{t+1}} \times \frac{y_t}{y_{t+1}} \\ &= \beta \left[ \frac{\eta_{t+1} + \delta_{t+1} x_{t+1}}{\eta_t + \delta_t x_t} \right] \frac{y_t}{y_{t+1}}, \end{aligned} \quad (\text{B.1})$$

where I have made use of the equilibrium budget relationship  $c_t/y_t = \eta_t/(\eta_t + \delta_t x_t)$  from equation (39).

Making use of equation (6), the term  $y_t/y_{t+1}$  in equation (B.1) can be written as

$$\frac{y_t}{y_{t+1}} = \frac{\exp(z_t) k_{n,t}^{\alpha_t} h_{1,t}^{1-\alpha_t}}{\exp(z_{t+1}) k_{n,t+1}^{\alpha_{t+1}} h_{1,t+1}^{1-\alpha_{t+1}}}, \quad (\text{B.2})$$

where  $k_{n,t} \equiv k_t \exp(-z_t)$  is the normalized capital stock, a stationary variable. Starting from equation (11), the law of motion for the normalized capital stock is given by

$$\begin{aligned} k_{n,t+1} &= \exp(z_t - z_{t+1}) B \exp(v_t) k_{n,t}^{1-\varphi_t} \left[ \frac{i_t y_t}{y_t k_t} \right]^{\delta_t} h_{2,t}^{\varphi_t}, \\ &= \exp(z_t - z_{t+1}) B \exp(v_t) k_{n,t}^{1-\varphi_t - \delta_t(1-\alpha_t)} \left[ \frac{\delta_t x_t}{\eta_t + \delta_t x_t} A h_{1,t}^{1-\alpha_t} \right]^{\delta_t} h_{2,t}^{\varphi_t}. \end{aligned} \quad (\text{B.3})$$

Equations (36) and (37) can be used to substitute for  $h_{1,t}$ ,  $h_{1,t+1}$ , and  $h_{2,t}$  in equations (B.2) and (B.3). Then, since  $x_t$  depends on the equilibrium solution for  $q_t$ , equation (34) can be used to make the substitutions  $x_t = x(\eta_t, \alpha_t, \delta_t, \varphi_t, s_t)$  and  $x_{t+1} = x(\eta_{t+1}, \alpha_{t+1}, \delta_{t+1}, \varphi_{t+1}, s_{t+1})$  in equations (B.1) through (B.3). After these various substitutions, a log-linear approximation of the stochastic discount factor takes the form

$$\begin{aligned} M_{t+1} &\simeq \beta \exp(-\mu) \left[ \frac{\eta_t}{\bar{\eta}} \right]^{m_1} \left[ \frac{\alpha_t}{\bar{\alpha}} \right]^{m_2} \left[ \frac{\delta_t}{\bar{\delta}} \right]^{m_3} \left[ \frac{\varphi_t}{\bar{\varphi}} \right]^{m_4} \left[ \frac{k_{n,t}}{\bar{k}_n} \right]^{m_5} \\ &\quad \times \exp[m_6 v_t + m_7 u_t + m_8 (s_t - \bar{s}) + m_9 \varepsilon_{\eta,t+1} + m_{10} \varepsilon_{\alpha,t+1}] \\ &\quad \times \exp[m_{11} \varepsilon_{\delta,t+1} + m_{12} \varepsilon_{\varphi,t+1} + m_{13} \varepsilon_{z,t+1} + m_{14} \varepsilon_{u,t+1} + m_{15} \varepsilon_{s,t+1}], \end{aligned} \quad (\text{B.4})$$

where  $m_1$  through  $m_{15}$  are Taylor series coefficients and the laws of motions for the shocks have been used to eliminate  $\eta_{t+1}$ ,  $\alpha_{t+1}$ ,  $\delta_{t+1}$ ,  $\varphi_{t+1}$ ,  $z_{t+1}$ ,  $u_{t+1}$ , and  $s_{t+1}$ . The steady state value of  $\bar{k}_n$  is given by  $k_t \exp(-\bar{z}_t)$  in 1972.Q3, where  $\bar{z}_t$  is the trend value of  $z_t$  constructed as  $\bar{z}_t = \bar{z}_{t-1} + \mu$  such that  $\mu$  is the sample mean of  $\Delta z_t$  and  $\bar{z}_t = z_t = 0$  in 1972.Q3. Given equation (B.4), it is straightforward to compute  $p_{b,t} = E_t^m M_{t+1}$  and  $r_{b,t} = 1/p_{b,t} - 1$ , where  $E_t^m$  is the model-consistent expectation based on orthogonal shocks.

The long-term bond pricing equation (23) can be approximated as follows

$$p_{c,t} \simeq E_t^m M_{t+1} (1 + \bar{\delta}_c \bar{p}_c) \left[ \frac{p_{c,t+1}}{\bar{p}_c} \right]^{b_c} \exp(b_c \omega_{t+1}), \quad (\text{B.5})$$

where  $b_c = \bar{\delta}_c \bar{p}_c / (1 + \bar{\delta}_c \bar{p}_c)$  is a Taylor series coefficient. A conjectured solution for equation (B.5) takes the form

$$p_{c,t} = \bar{p}_c \left[ \frac{\eta_t}{\bar{\eta}} \right]^{n_1} \left[ \frac{\alpha_t}{\bar{\alpha}} \right]^{n_2} \left[ \frac{\delta_t}{\bar{\delta}} \right]^{n_3} \left[ \frac{\varphi_t}{\bar{\varphi}} \right]^{n_4} \left[ \frac{k_{n,t}}{\bar{k}_n} \right]^{n_5} \exp [n_6 v_t + n_7 u_t + n_8 (s_t - \bar{s}) + n_9 \omega_t]. \quad (\text{B.6})$$

The conjectured solution (B.6) is iterated ahead one period and then substituted into the approximated long-term bond pricing equation (B.5) together with the expression for  $M_{t+1}$  from equation (B.4). Collecting terms and then evaluating the model-consistent expectation yields a set of ten equations in the ten solution coefficients given by  $\bar{p}_c$  and  $n_1$  through  $n_9$ . The value of  $\bar{p}_c$  depends on the coupon decay parameter  $\bar{\delta}_c$  and numerous shock variances. Given the shock variances, I solve for the value of  $\bar{\delta}_c$  such that  $p_{c,t} = \bar{p}_c = 20$  in 1972.Q3. The target value of  $\bar{p}_c$  is arbitrary and has no affect on the model-implied sequence for the long-term bond return, as given by  $r_{c,t} = [1 + \bar{\delta}_c \exp(\omega_t) p_{c,t}] / p_{c,t-1} - 1$ .

## C Shock identification procedure

The sequence for the factor distribution shock  $\alpha_t$  is directly pinned down by U.S. data on capital's share of income. Data for U.S. total hours worked per person  $h_t$  are plotted in Figure 2. By equating the right-sides of the two equilibrium conditions (16) and (17), the model-implied sequences for  $h_{1,t}$  and  $h_{2,t}$  are constructed using the following equations

$$h_{1,t} = h_t [1 + (\varphi_t / \delta_t) (i_t / y_t) / (1 - \alpha_t)]^{-1} = h_t \left[ \frac{(1 - \alpha_t) y_t}{y_t - d_t - i_t} \right], \quad (\text{C.1})$$

$$h_{2,t} = h_t - h_{1,t} = h_t \left[ \frac{\alpha_t y_t - d_t - i_t}{y_t - d_t - i_t} \right], \quad (\text{C.2})$$

where I have made use of  $w_t = (1 - \alpha_t) y_t / h_{1,t}$  and  $d_t = \alpha_t y_t - (1 + \varphi_t / \delta_t) i_t$ . The right-side values of  $\alpha_t$ ,  $h_t$ ,  $y_t$ ,  $d_t$ , and  $i_t$  in equations (C.1) and (C.2) are given by the U.S. data plotted in Figure 2.

Given the model-implied sequences for  $h_{1,t}$  and  $h_{2,t}$ , the sequences for the shocks  $z_t$ ,  $\delta_t$ ,  $\varphi_t$  and  $v_t$  are uniquely pinned down using the following equations:

$$z_t = [\log(y_t) - \log(A k_t^{\alpha_t} h_{1,t}^{1-\alpha_t})] / (1 - \alpha_t), \quad (\text{C.3})$$

$$\delta_t = i_t / p_{s,t}, \quad (\text{C.4})$$

$$\varphi_t = \delta_t (\alpha_t y_t - d_t - i_t) / i_t \quad (\text{C.5})$$

$$v_t = \log(k_{t+1} / k_t) - \log(B) - \delta_t \log(i_t / k_t) + \varphi_t \log[k_t \exp(-z_t) / h_{2,t}], \quad (\text{C.6})$$

where the right-side values of the macroeconomic variables are given by the U.S. data plotted in Figure 2. If a shock appears on the right side, then it takes on the value identified in a previous equation.<sup>41</sup>

The sequences for the shocks  $u_t$ ,  $s_t$ , and  $\eta_t$  are determined iteratively by solving the following set of simultaneous equations

$$u_t = \log \{ \eta_t (1 - \alpha_t) / [(c_t / y_t) Dh_{1,t} h_t^\gamma] \}, \quad (\text{C.7})$$

$$s_t = \bar{s} - (1/\rho_s) (\bar{s} + \sigma_{\varepsilon,s}^2/2) + (1/\rho_s) \log [\eta_t (p_{s,t}/c_t) / (\beta E_t^m q_{t+1}^f)], \quad (\text{C.8})$$

$$\begin{aligned} \eta_t = & \bar{\eta} \{ p_{b,t} \beta^{-1} \exp(\mu) [\alpha_t / \bar{\alpha}]^{-m_2} [\delta_t / \bar{\delta}]^{-m_3} [\varphi_t / \bar{\varphi}]^{-m_4} [k_{n,t} / \bar{k}_n]^{-m_5} \\ & \times \exp [-m_6 v_t - m_7 u_t - m_8 (s_t - \bar{s}) - m_9 \sigma_{\varepsilon,\eta}^2/2 - m_{10} \sigma_{\varepsilon,\alpha}^2/2 - m_{11} \sigma_{\varepsilon,\delta}^2/2] \\ & \times \exp [-m_{12} \sigma_{\varepsilon,\varphi}^2/2 - m_{13} \sigma_{\varepsilon,z}^2/2 - m_{14} \sigma_{\varepsilon,u}^2/2 - m_{15} \sigma_{\varepsilon,s}^2/2] \}^{1/m_1}, \end{aligned} \quad (\text{C.9})$$

where equation (C.7) is the equilibrium labor supply condition (35), equation (C.8) is the equity market first order condition (24), and equation (C.9) is the short-term bond pricing equation (22) that determines the value of  $p_{b,t}$  at the start of quarter  $t$ . I assume that  $p_{b,t}$  in the data is given by the inverse of the U.S. gross risk free rate of return computed from the start of quarter  $t$  to the end of quarter  $t$ . The model-consistent, fundamentals-only forecast  $E_t^m q_{t+1}^f$  that appears in equation (C.8) is computed using the fundamental solution (26). The fundamentals-only forecast depends on the shocks  $\eta_t$ ,  $\alpha_t$ ,  $\delta_t$ , and  $\varphi_t$  which are determined from equations (C.3) through (C.9).

Various parameters and shock variances that appear in equations (C.8) and (C.9) are initially undetermined, but influence the computed sequences for  $u_t$ ,  $s_t$ , and  $\eta_t$ . These parameters and shock variances include  $\bar{s}$ ,  $\beta$ ,  $\rho_s$ ,  $\sigma_{\varepsilon,s}$ ,  $\sigma_{\varepsilon,\eta}$ , and  $\sigma_{\varepsilon,u}$ . Starting from initial guesses for these parameter values and shock variances, together with initial guesses for the sequences of  $u_t$ ,  $s_t$ , and  $\eta_t$ , equations (C.7) through (C.9) are iterated until convergence is achieved. After each iteration, new guesses for the sequences of  $u_t$ ,  $s_t$  and  $\eta_t$  are computed as an exponentially-weighted moving average of the current and past sequences of shock realizations implied by equations (C.7) through (C.9). In practice, convergence to 8 decimal places takes around 50 iterations.

To identify the bond coupon decay rate shock  $\omega_t$ , I first solve the equilibrium bond price solution (B.6) for  $\exp(\omega_t)$ , yielding

$$\begin{aligned} \exp(\omega_t) = & \{ [p_{c,t}/\bar{p}_c] [\eta_t/\bar{\eta}]^{-n_1} [\alpha_t/\bar{\alpha}]^{-n_2} [\delta_t/\bar{\delta}]^{-n_3} [\varphi_t/\bar{\varphi}]^{-n_4} [k_{n,t}/\bar{k}_n]^{-n_5} \\ & \times \exp [-n_6 v_t - n_7 u_t - n_8 (s_t - \bar{s})] \}^{1/n_9}, \end{aligned} \quad (\text{C.10})$$

where  $p_{c,t} = \bar{p}_c$  in 1972.Q3 such that  $\omega_t = 0$ . Next, I substitute equation (C.10) into the definition of the gross bond return given by  $1 + r_{c,t} = [1 + \bar{\delta}_c \exp(\omega_t) p_{c,t}] / p_{c,t-1}$  and then solve

---

<sup>41</sup>Since the computation of  $v_t$  requires data at time  $t+1$ , I set the end-of-sample shock value to  $v_T = \rho_v v_{T-1}$ , where  $T = 2022.Q4$ .

for  $p_{c,t}$ . This procedure yields

$$p_{c,t} = \left\{ \bar{p}_c [p_{c,t-1} (1 + r_{c,t}) / \bar{\delta}_c - 1 / \bar{\delta}_c]^{n_9} [\eta_t / \bar{\eta}]^{n_1} [\alpha_t / \bar{\alpha}]^{n_2} [\delta_t / \bar{\delta}]^{n_3} [\varphi_t / \bar{\varphi}]^{n_4} [k_{n,t} / \bar{k}_n]^{n_5} \right. \\ \left. \times \exp [n_6 v_t + n_7 u_t + n_8 (s_t - \bar{s})] \right\}^{1/(1+n_9)}, \quad (\text{C.11})$$

where  $1 + r_{c,t}$  is the U.S. gross real bond return in quarter  $t$ . Given the sequences for the previously-identified shocks, equation (C.11) is used to construct the equilibrium sequence for  $p_{c,t}$  for  $t > 1972.Q3$ , starting with  $p_{c,t-1} = \bar{p}_c$ . For  $t < 1972.Q3$ , equation (C.11) is inverted to solve for  $p_{c,t-1}$  as a function of  $p_{c,t}$  and the previously-identified shocks.

Given the equilibrium sequence for  $p_{c,t}$  from 1960.Q1 to 2022.Q4, equation (C.10) is used to recover the model-implied sequence for  $\exp(\omega_t)$ . The stochastic coupon decay rate is given by  $\delta_{c,t} \equiv \bar{\delta}_c \exp(\omega_t)$ .

After each iteration of the shock identification exercise, the parameters governing the persistence and volatility of the model-implied shocks are recomputed using the shock sequences obtained from the previous iteration. The persistence parameters are computed by running an OLS regression on the univariate law of motion for the shock where the constant term in the regression is constrained to coincide with the model steady state value in 1972.Q3.

## D Data sources and methods

I start with data on nominal personal consumption expenditures on nondurable goods plus services ( $C_t$ ), nominal private nonresidential fixed investment plus nominal personal consumption expenditures on durable goods ( $I_t$ ), the corresponding chain-type price indices for each of the various nominal expenditure categories that sum to  $C_t$  and  $I_t$ , and U.S. population. All of this data are from the Federal Reserve Bank of St. Louis' FRED database. I define the nominal ratios  $C_t/Y_t$  and  $I_t/Y_t$ , where  $Y_t \equiv C_t + I_t$ . The nominal ratios capture shifts in relative prices. I deflate  $Y_t$  by an output price index constructed as the weighted-average of the chain-type price indices for each of the various nominal expenditure categories that sum to  $C_t$  and  $I_t$ . The weights each period are the categories' nominal expenditure ratios relative to  $Y_t$ . After dividing by U.S. population, the level of real output per person  $y_t$  is normalized to 1.0 in 1972.Q3. The real per person series for  $c_t$  and  $i_t$  are then constructed by applying the nominal ratios  $C_t/Y_t$  and  $I_t/Y_t$  to the constructed  $y_t$  series. In this way, the real per person series for  $c_t$  and  $i_t$  reflect the same resource allocation ratios as the nominal per person series.

Data for  $h_t$  are hours worked of all persons in the nonfarm business sector from FRED, divided by U.S. population and then normalized to equal 0.3 in 1972.Q3.<sup>42</sup>

The data for  $k_t$  are constructed using the historical-cost net stock of private nonresidential fixed assets plus the historical-cost net stock of consumer durable goods, both in billions of dollars at year end, from the Bureau of Economic Analysis (BEA), NIPA Table 4.3, line 1

<sup>42</sup>The hours data are from <https://fred.stlouisfed.org/series/HOANBS>.

and Table 8.3, line 1, respectively. The data are only available at annual frequency, so I first create a quarterly series by log-linear interpolation. The nominal capital stock series is deflated using the output price index described above and then divided by U.S. population. I normalize the real per person series for  $k_t$  to deliver a target value of  $i_t/k_t = 0.031$  in 1972.Q3. The target value is arbitrary given that the model parameters  $B$  and  $\bar{\delta}$  can be adjusted to hit any desired target value. I choose the target value of  $i_t/k_t$  to coincide with the steady state value implied by a model with no capital adjustment costs, such that  $i_t/k_t = k_{t+1}/k_t - 1 + \delta'$ , where  $k_{t+1}/k_t = \exp(0.006)$  is the mean quarterly growth rate of the real capital stock per person series described above and  $\delta' = 0.025$  is a typical quarterly depreciation rate.

I calibrate the value of  $A$  in the production function (6) to yield  $y_t = 1$  in 1972.Q3 when  $k_t$  is equal to the normalized capital stock and  $z_t = 0$  in 1972.Q3. This procedure yields  $A = 0.9989$  and a sample mean of  $k_t/y_t = 9.190$  from 1960.Q1 to 2022.Q4.

Following Lansing (2015) and Lansing and Markiewicz (2018), capital's share of income is measured as one minus the ratio of employee compensation to gross value added of the corporate business sector. Both series are from the BEA, NIPA Table 1.14, lines 1 and 4.

To construct data for  $p_{s,t}$ , I start with the nominal market capitalization of the S&P 500 stock index from [www.siblisresearch.com](http://www.siblisresearch.com). The nominal market capitalization is deflated using the output price index described above and then divided by U.S. population to create a series for real equity value per person.

Quarterly data on the nominal end-of-quarter closing value of the S&P 500 stock index, nominal dividends, the nominal risk free rate of return (based on a 3-month Treasury bill), and the nominal return on a long-term Treasury bond (based on a maturity of approximately 20 years) are from Welch and Goyal (2008).<sup>43</sup> The gross nominal return on the S&P 500 stock index in quarter  $t$  is defined as  $(P_t + D_t/4)/P_{t-1}$ , where  $P_t$  is the end-of-quarter closing value of the index and  $D_t$  is cumulative nominal dividends over the past 4 quarters. Gross nominal asset returns are converted to gross real returns by dividing by  $1 + \pi_t$  where  $\pi_t$  is the quarterly inflation rate computed using the output price index described above.<sup>44</sup> Given the gross real equity return  $1 + r_{s,t}$  and the constructed data for real equity value per person  $p_{s,t}$ , I compute a consistent series for real dividends per person as  $d_t = (1 + r_{s,t})p_{s,t-1} - p_{s,t}$ . The gross nominal returns on the 3-month Treasury bill and the long-term Treasury bond are similarly divided by  $1 + \pi_t$  to obtain the gross real bond returns  $1 + r_{b,t}$  and  $1 + r_{c,t}$ .

The consumer sentiment series plotted in Figure 1 is from the University of Michigan's Survey of Consumers.<sup>45</sup> The survey data on investors' expected stock returns over the next year is from Nagel and Xu (2022a).<sup>46</sup> The series is constructed by combining information from

---

<sup>43</sup>Updated data through the end of 2022 are available from Amit Goyal's website: <https://sites.google.com/view/agoyal145>.

<sup>44</sup>The correlation coefficient between  $\pi_t$  and the quarterly inflation rate computed using the personal consumption expenditures (PCE) price index is 0.9.

<sup>45</sup>See [www.sca.isr.umich.edu/tables.html](http://www.sca.isr.umich.edu/tables.html).

<sup>46</sup>The data are available from <https://voices.uchicago.edu/stefannagel/code-and-data/>.

the UBS/Gallup survey, the Conference Board survey, the University of Michigan’s Survey of Consumers, plus several smaller surveys of brokerage and investment firm customers.

## E Forecast accuracy comparison

The boundedly-rational agent in the model employs univariate forecast rules for each of the nine shocks. Under full information rational expectations, the agent would employ forecast rules that capture the complex correlation structure in Table 5. As detailed in Appendix C, the five shocks  $\alpha_t$ ,  $z_t$ ,  $v_t$ ,  $\delta_t$ , and  $\varphi_t$  are identified directly from the data or from model equilibrium conditions that do not involve the agent’s conditional forecasts. The remaining four shocks  $s_t$ ,  $\eta_t$ ,  $u_t$ , and  $\omega_t$  are identified from model equilibrium conditions that do involve the agent’s conditional forecasts, so the assumption of bounded-rationality has some influence the resulting sequences for these four shocks.

Table E.1 examines the potential improvement in forecast accuracy from taking into account the complex shock correlation structure. Specifically, I compare the accuracy of the model’s univariate forecast rules to the accuracy of forecasts derived from a 1-lag VAR estimated on the nine model-identified shock sequences for the period 1960.Q3 to 2022.Q4. Both sets of forecast rules are obtained by running ordinary least squares (OLS) regressions in which the constant terms are constrained to coincide with the steady state or trend values of the shocks in 1972.Q3. For all nine shocks, use of the VAR improves forecast accuracy by less than 9% as measured by the mean absolute forecast error (MAFE). The last column of Table E.1 shows that the univariate shock forecasts are almost perfectly correlated with the VAR shock forecasts. These results confirm that the univariate forecast rules are near rational.

Table E.1: 1-Quarter-Ahead Shock Forecasts

Forecast Object	Univariate MAFE	VAR MAFE	VAR Improvement	Forecast Correlation
$s_{t+1} - \bar{s}$	0.0750	0.0724	-3.37%	0.987
$\log(\eta_{t+1}/\bar{\eta})$	0.0933	0.0872	-6.60%	0.974
$u_{t+1}$	0.0966	0.0895	-7.29%	0.973
$v_{t+1}$	0.0257	0.0254	-1.45%	0.998
$\log(\delta_{t+1}/\bar{\delta})$	0.0624	0.0595	-4.70%	0.999
$\log(\varphi_{t+1}/\bar{\varphi})$	0.0991	0.0951	-4.02%	0.998
$\log(\alpha_{t+1}/\bar{\alpha})$	0.0096	0.0089	-7.41%	0.996
$\Delta z_{t+1} - \mu$	0.0164	0.0156	-4.74%	0.999
$\omega_{t+1}$	0.0047	0.0043	-8.55%	0.995

Notes: MAFE = mean absolute forecast error. Univariate forecasts are computed using the shock parameters in Tables 1 and 2. The VAR forecasts are computed from a 1-lag VAR estimated on the model-identified shocks with constant terms in the regression constrained to coincide with the steady state shock values in 1972.Q3.

Table E.2 examines the potential improvement in forecast accuracy from an ex post OLS regression that projects each model forecast object in period  $t + 1$  onto the relevant model state variables in period  $t$ . The three model forecast objects are  $q_{t+1}$ ,  $M_{t+1}$ , and  $q_{c,t+1} \equiv M_{t+1}[1 + \bar{\delta}_c \exp(\omega_{t+1}) p_{c,t+1}]$  which appear in the three equilibrium conditions (25), (22), and (23). The mean values of these forecast objects from 1960.Q2 to 2022.Q4 are 4.943, 1.000, and 31.65, respectively. The relevant model state variables are those included in the corresponding model forecasts which are computed as described in Appendices A and B. As in the model, the constant terms in the ex post OLS regressions are constrained to coincide with the steady state or trend values of the model state variables in 1972.Q3. The OLS regressions represent the best the agent can do in exploiting any cross correlations between the relevant model state variables when forecasting  $q_{t+1}$ ,  $M_{t+1}$ , or  $q_{c,t+1}$ . In the case of all three forecast objects, use of the ex post OLS regressions improves forecast accuracy by less than 8% as measured by the MAFE.

Table E.2: 1-Quarter-Ahead Model Forecasts

Forecast Object	Model MAFE	OLS MAFE	OLS Improvement
$q_{t+1}$	0.571	0.555	-2.78%
$M_{t+1}$	0.092	0.085	-7.44%
$q_{c,t+1}$	3.64	3.37	-7.41%

Notes: MAFE = mean absolute forecast error. Model forecasts are computed as described in Appendices A and B. The OLS projection forecasts are computed by regressing each forecast object on the relevant model state variables in period  $t$  with constant terms constrained to coincide with the model steady state values in 1972.Q3.

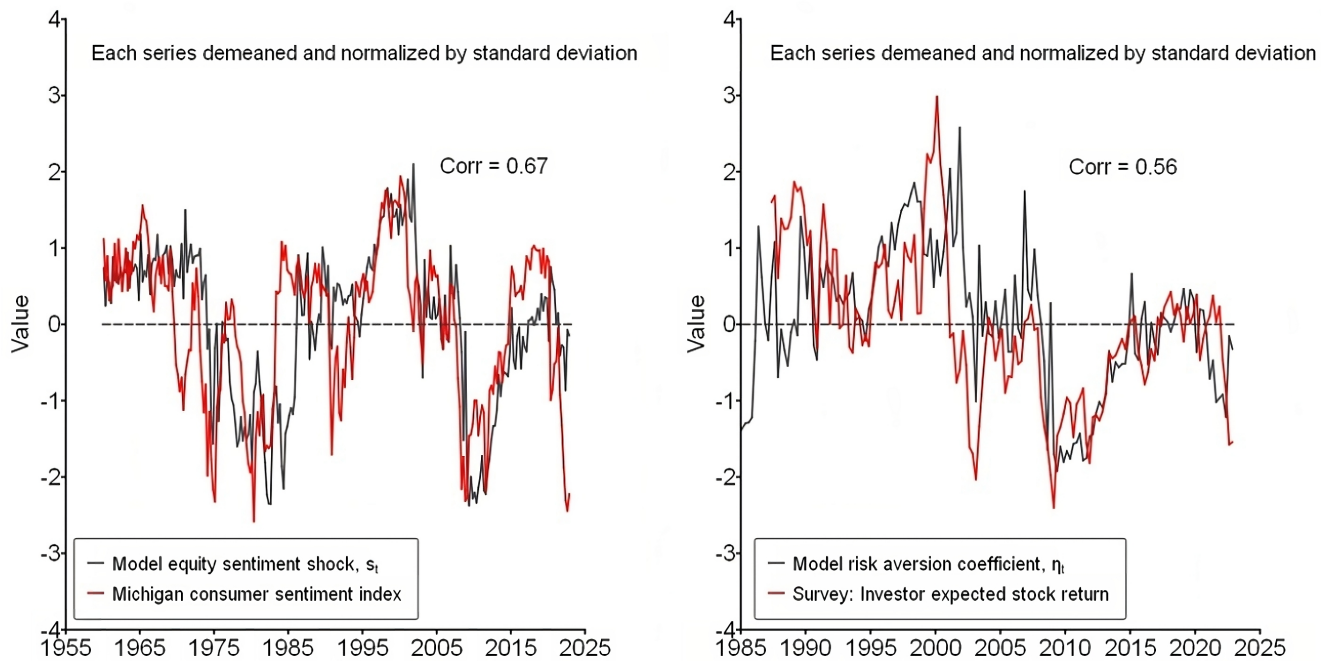


Figure 1: Model-identified sentiment and risk aversion

Notes: The model-identified sentiment shock (left panel) is strongly correlated with the University of Michigan's consumer sentiment index (which is not used in the shock identification procedure). The model-identified risk aversion coefficient (right panel) is strongly correlated with a survey-based measure of investors' expected stock returns over the next year from Nagel and Xu (2022a). Data series are described in Appendix D.

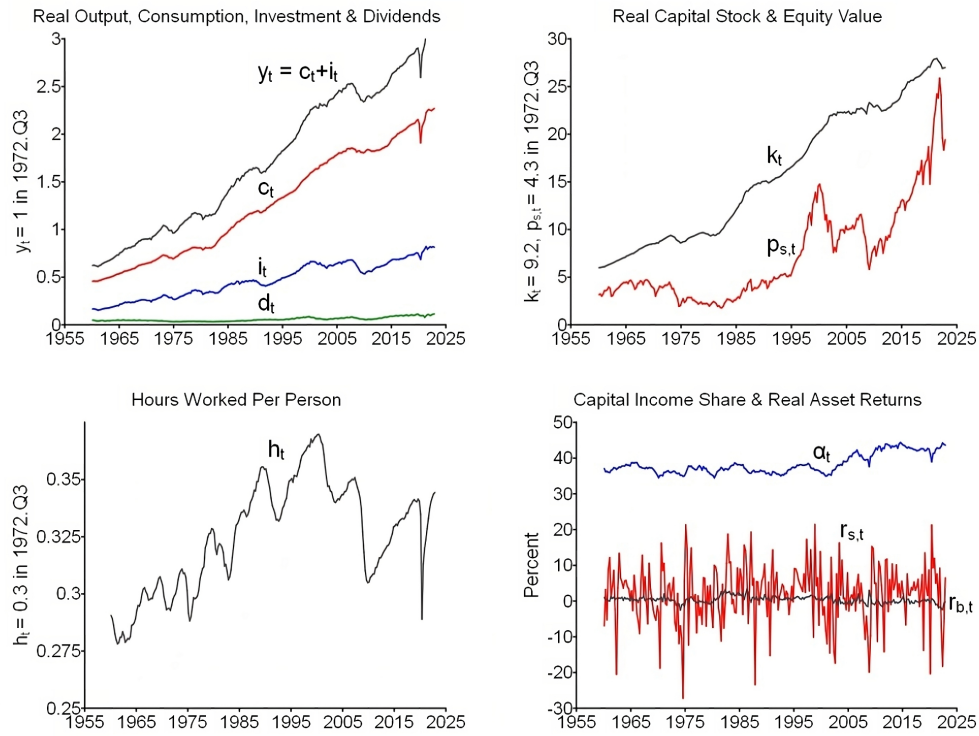


Figure 2: U.S. macroeconomic variables and asset returns

Notes: The baseline model exactly replicates the quarterly time paths of all ten U.S. variables plotted above plus the real return on a long-term U.S. Treasury bond from 1960 to 2022. Data series are described in Appendix D.

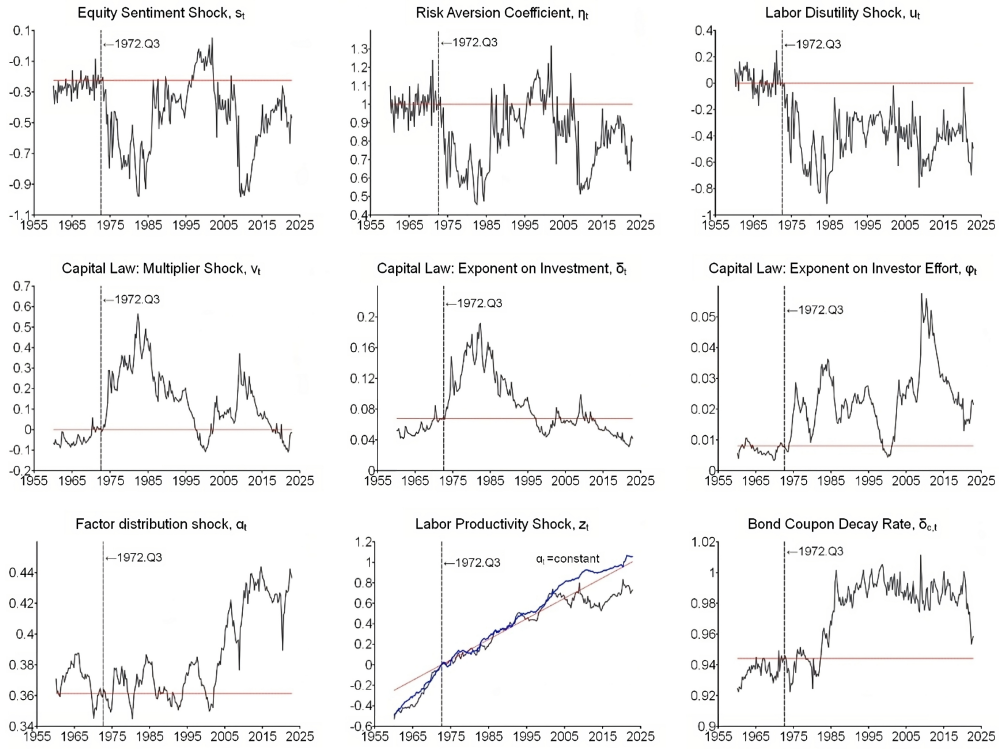


Figure 3: Model-identified shocks

Notes: The equity sentiment shock is strongly correlated with the time-varying risk aversion coefficient  $\eta_t$  and the labor disutility shock  $u_t$ . The three capital law of motion shocks  $v_t$ ,  $\delta_t$ , and  $\varphi_t$  are strongly correlated with each other. Innovations to the factor distribution shock  $\alpha_t$  are negatively correlated with innovations to the labor productivity shock  $z_t$ . These patterns motivate three categories of shocks for the counterfactual scenarios: (1) only sentiment and preference shocks, (2) only capital law of motion shocks, and (3) only production function shocks. The bottom middle panel plots an alternative sequence for  $z_t$  that is identified by an otherwise similar model with  $\alpha_t = \bar{\alpha}$  for all  $t$ .

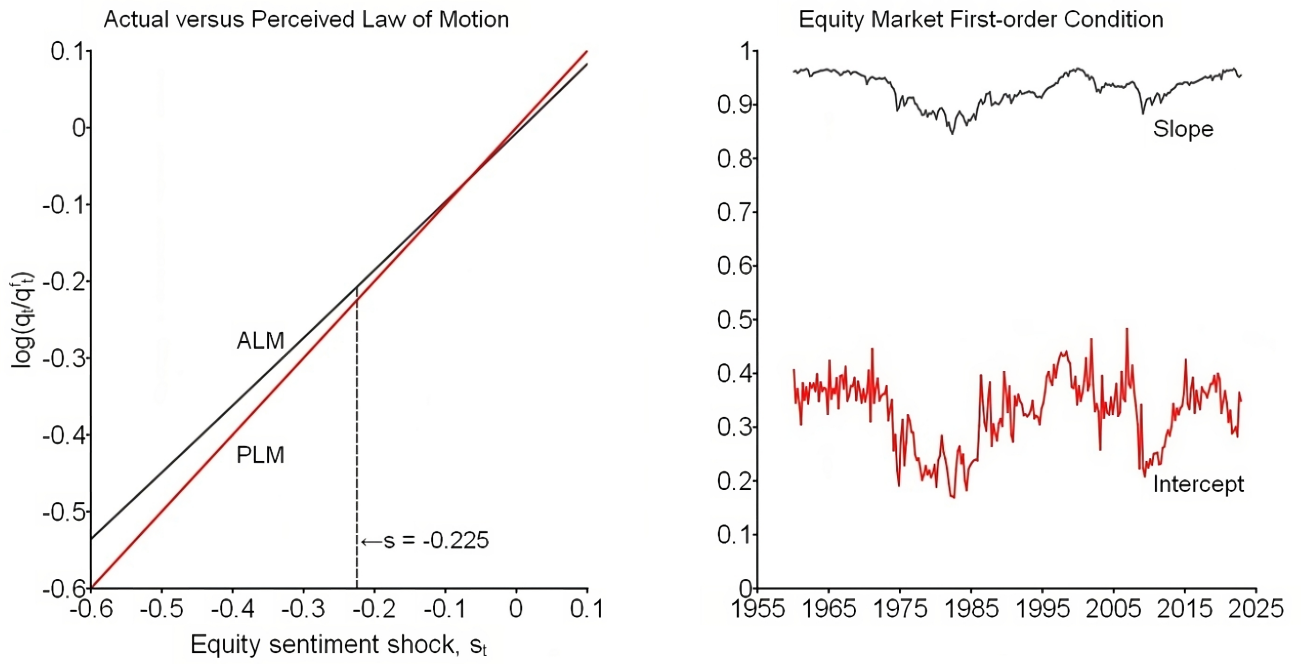


Figure 4: Actual versus Perceived Law of Motion

Notes: The agent's perceived law of motion (28) predicts values for the quantity  $\log(q_t/q_t^e)$  that are numerically very close to those generated by the actual law of motion. This is because the slope of the equity market first order condition (25) is always close to 1. Consequently, the agent's perception that equity value is partly driven by sentiment is close to self-fulfilling.

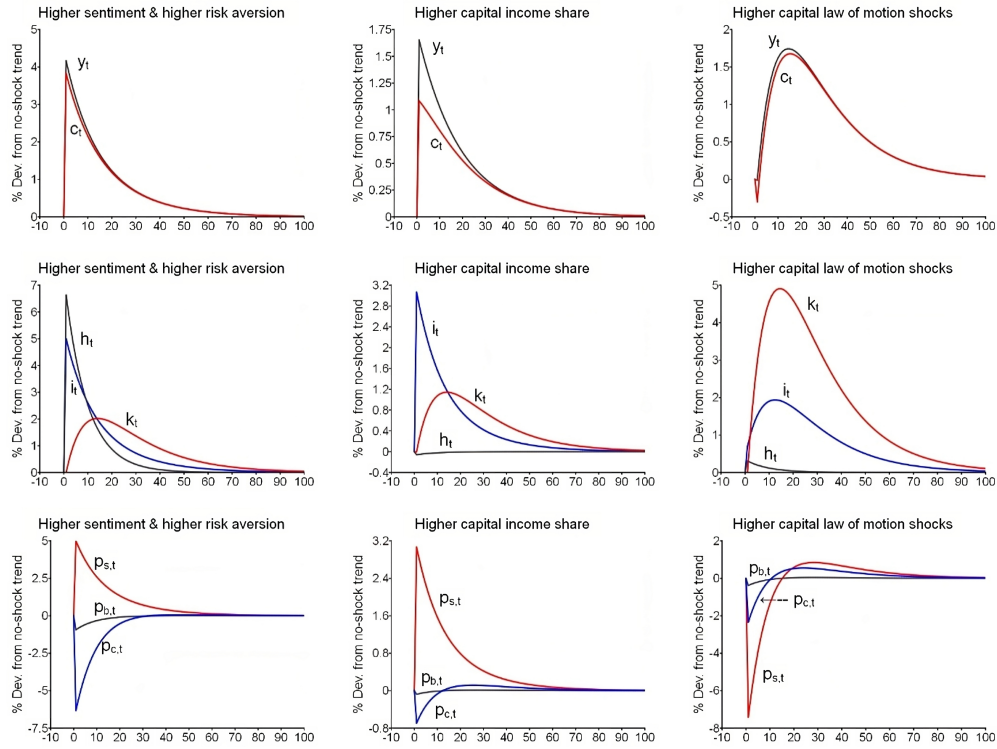


Figure 5: Impulse response functions

Notes: Positive innovations to each of the three main shock categories can generate all or most of the features of a typical business cycle. Higher sentiment together with higher risk aversion (left panels) produces a correlated increase in macroeconomic variables. Equity value increases but bond prices decline, implying an increase in bond yields. A higher capital income share (middle panels) delivers a similar response pattern except that hours worked now undergoes a small decline. Higher values for the three capital law of motion shocks (right panels) also leads to a correlated increase in macroeconomic variables but equity value now declines together with bond prices.

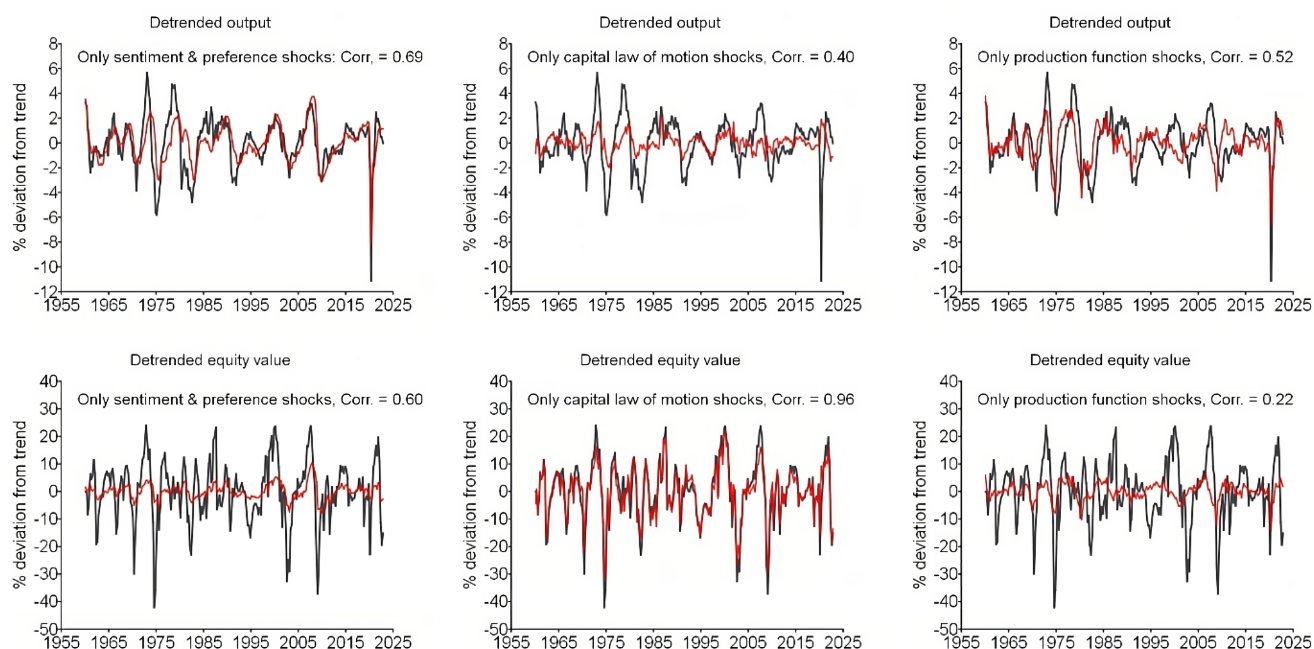


Figure 6: Importance of shock categories for detrended output and equity value

Notes: The panels compare the detrended paths of model output and model equity value (red lines) to the corresponding U.S. data (black lines) under three different shock scenarios. A large positive correlation coefficient implies that a given category of shocks is an important driver of business cycle movements in the U.S. variable. For detrended output, the correlation coefficients range from 0.40 to 0.69. For detrended equity value, the correlation coefficients range from 0.22 to 0.96. These results confirm that business cycle movements in U.S. output and equity value can be plausibly driven by multiple types of shocks.

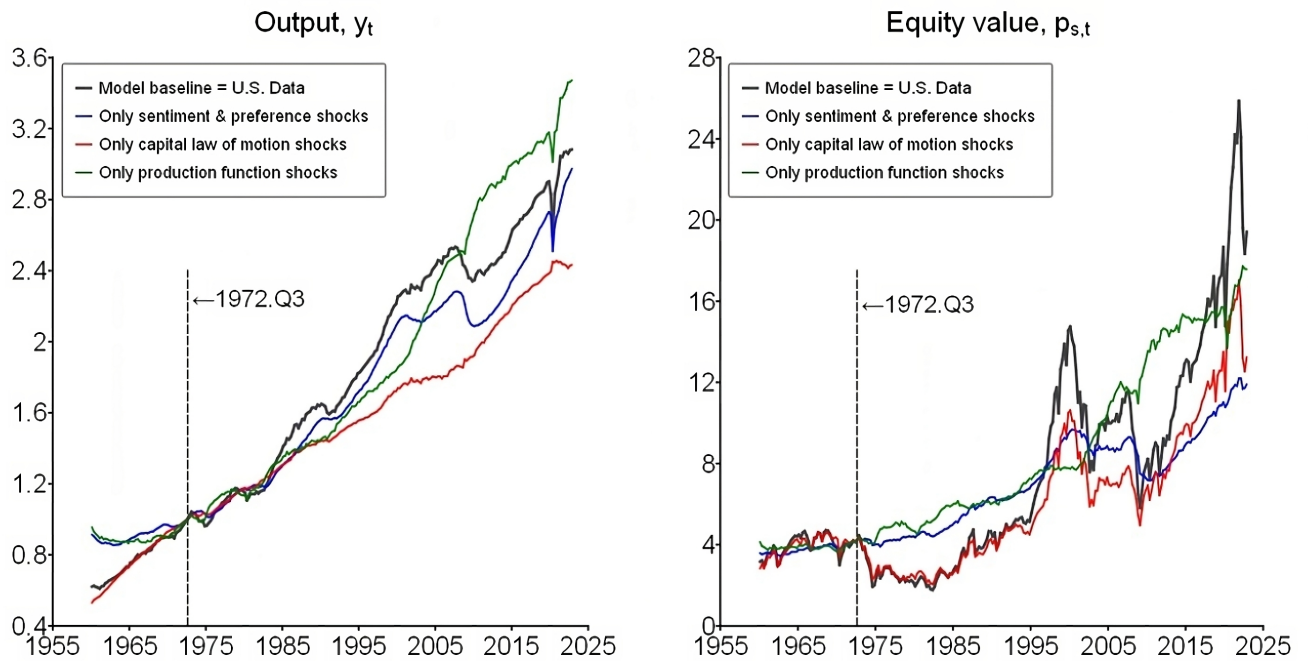


Figure 7: Counterfactual shock scenarios

Notes: Each counterfactual scenario adds one category of shock realizations (as indicated) while other shocks are set equal to steady state or trend values. The scenario with only sentiment and preference shocks (blue line) provides the best fit of fluctuations in U.S. output (left panel). The scenario with only the capital law of motion shocks (red line) provides the best fit of fluctuations in U.S. equity value (right panel).

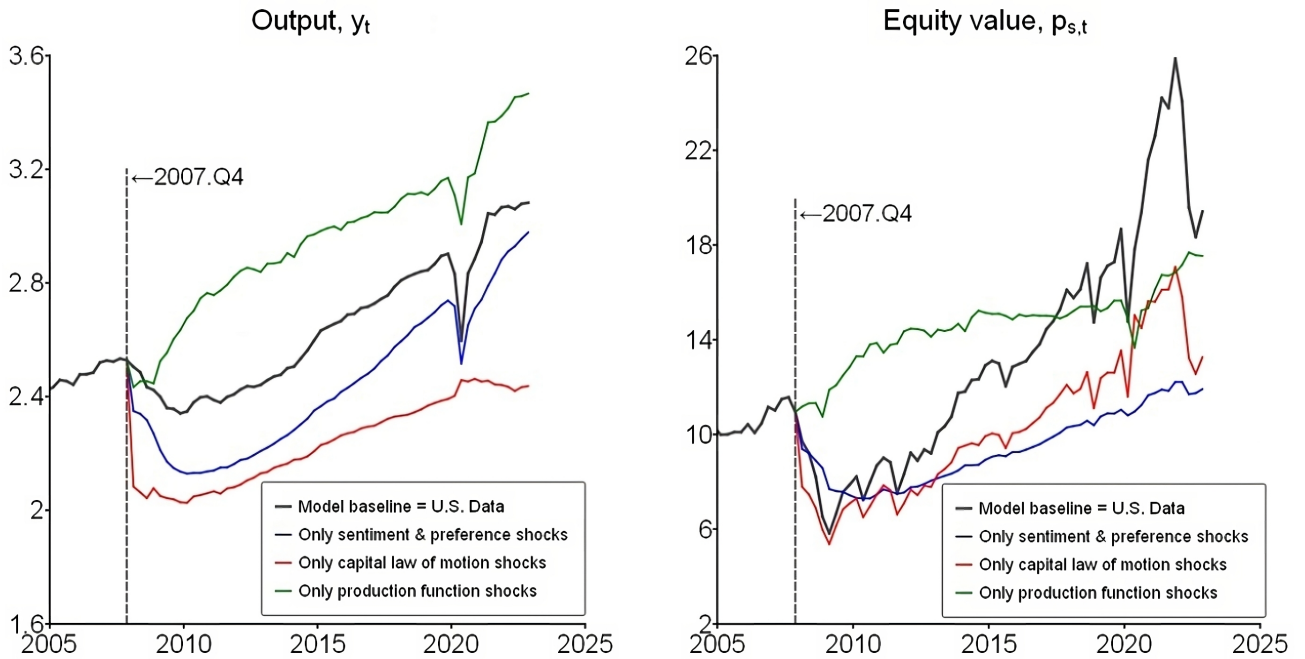


Figure 8: Great Recession versus Covid recession

Notes: According to the model, the declines in  $y_t$  and  $p_{s,t}$  during the Great Recession (2007.Q4 to 2009.Q2) are driven mainly by the capital law of motion shocks (red line) together with the sentiment and preference shocks (blue line). The production function shocks do not contribute much to the declines in either U.S. variable during this episode. The decline in  $y_t$  during the Covid recession (2019.Q4 to 2020.Q2) is driven mainly by the sentiment and preference shocks (blue line) together with production function shocks (green line). The decline in  $p_{s,t}$  during the Covid recession is driven mainly by capital law of motion shocks (red line) together with production function shocks (green line). Overall, the results tell us that U.S. recessions can be driven by different types of shocks.